

Galvanic vestibular stimulation elicits consistent neck motion in seated subjects

MSc Thesis

Farzad Ehtemam

Supervisors:

Dr. Ir. Riender Happee

Dr. Ir. Alfred C. Schouten

Ir. Patrick A. Forbes

Farzad Ehtemam

Student Number: 1388193

Graduation Date: 29 August 2011

Institute: Delft University of Technology

Faculty of Mechanical, Maritime and Materials Engineering

Department of BioMedical Engineering

Board of Examiners:

Prof. Dr. F.C.T. van der Helm (3mE, BMechE)

Dr. Ir. R. Happee (3mE, BMechE)

Dr. Ir. A.C. Schouten (3mE, BMechE)

P.A. Forbes, MASc (3mE, BMechE)

Dr. Ir. M.M. van Paassen (L&R, Control & Simulation)

Contents

Contents.....	3
Introduction	5
Methods.....	6
Subjects.....	6
Apparatus.....	6
Stimuli	8
Protocol.....	9
Analysis	9
Data processing	9
Non-parametric system identification	10
Statistics.....	11
Results	12
Response effects due to time	12
Responses in frequency domain.....	14
Auto-spectral densities	14
Transfer functions and coherences.....	16
Multisine vs. single sine	19
Non-vestibular stimulation	19
Discussion.....	20
Coherent motion.....	20
Response characteristics.....	20
Subject variability and reliability.....	21
Limitations.....	22
Conclusions.....	22
Future work.....	22
References	24
Appendix A – Statistical tables.....	28
Appendix B – Results for all subjects.....	37
Appendix C – EMG measurements and analysis.....	54

Galvanic vestibular stimulation elicits consistent neck motion in seated subjects

Farzad Ehtemam¹, Patrick A. Forbes¹, Alfred C. Schouten^{1,2}, Riender Happee¹, Herman Kingma³, Frans C. T. van der Helm^{1,2}

¹Department of BioMechanical Engineering, Delft University of Technology, 2628 CD Delft, The Netherlands

²Laboratory of Biomechanical Engineering, MIRA Institute for Biomedical Technology and Technical Medicine, University of Twente, P.O. Box 217, 7500 AE Enschede, The Netherlands

³Department of Otorhinolaryngology—Head and Neck Surgery, University Hospital Maastricht, P. Debeyelaan 25, Maastricht 6229, The Netherlands

Abstract

Galvanic vestibular stimulation (GVS) alters the firing rates of vestibular afferents and consequently provokes the illusion of movement. In standing balance GVS is used to assess the contribution of the vestibular system, where it has been shown to elicit coherent responses in lower extremity muscles involved in maintaining balance. However, to date no information exists regarding the influence of GVS on neck muscles or head-neck stabilization. This study aims to test the hypothesis that GVS can be used as a technique to investigate the vestibular contribution to head and neck stabilization. Sinusoidal stimuli of 0.5 – 2 mA within the bandwidth of 0.4 – 5.2 Hz were used as GVS signals and applied to eleven healthy subjects using a bilateral bipolar configuration. Subjects were blindfolded and stimulated while seated on and restrained to a chair. Measurements of natural sway (without stimulation) were included as control trials. Displacements of head and torso were recorded using a motion capture system. System identification techniques were used to identify the relationship between the input (GVS) and the output (motion) of the head and neck. The results show significant coherence between GVS and the head-neck kinematics and modulation of these responses was observed across frequency and not amplitude, demonstrating the linear range of the vestibular feedback. Furthermore, the vestibular origin of the responses was demonstrated using non-vestibular stimulation tests. EMG measurements were used to characterize the relationship between the vestibular input and muscle activities in neck. Based on the findings of this study we propose that using GVS with system identification techniques provides a viable approach to quantify small motions (~ 0.1 mm) in neck and understand motion control of the head-neck.

Keywords: Galvanic vestibular stimulation, head stabilization, spatial perception, neck reflexes and system identification

Introduction

To stabilize the head and neck on the trunk, the central nervous system (CNS) needs kinematic information of the head, including orientation, velocity and acceleration (linear and angular) relative to the global coordinate frame of the external space. This information is provided through multiple sensory sources: visual, proprioceptive and vestibular. The vestibular system is multisensory and sends constant rotational (via the semicircular canals) and translational (via the otoliths) information about the orientation of the head relative to the outside world to the higher processing units. This information converges with the visual and proprioceptive signals at the vestibular nucleus (VN) in the brainstem to form the perception of spatial orientation of the head. The VN innervates the motor neurons controlling ocular, cervical and postural muscles (Purves *et al.*, 2008) and through neural pathways to these muscles, the vestibular reflexes contribute to stabilization tasks. This integrative nature of the system makes it difficult to isolate the contribution of the vestibular responses.

Early attempts to understand the mechanisms underlying control of head and neck used sinusoidal and impulsive forces applied directly to the head in the sagittal plane (Viviani & Berthoz, 1975). It was concluded that the system behaves as a quasi-linear second order system with two degrees of freedom. However, the results could not provide insight into the nature of different sensory systems involved in the control task. Additional studies have hypothesized that the involvement of different mechanisms in the control of head and neck depends on the frequency of the perturbation (Keshner *et al.*, 1995; Keshner & Peterson, 1995). These mechanisms were categorized as the voluntary motion, the vestibulocollic (VCR) and cervicocollic (CCR) reflexes and the head and neck mechanics. Random appearing perturbations were applied to the trunk of seated subjects and transfer functions (i.e. gain and phase) described the input-output relationship of platform motion with head angular velocity and neck EMG. The authors reported the reflexes (VCR and CCR) being dominant mechanisms for compensation in the frequency range between 1 and 2 Hz. However, the contribution of the VCR and CCR could not be separated. To date no agreement has been reached on the vestibular contribution to the control of head and neck.

A drawback to these studies is the use of mechanical stimuli, which not only disturbs the vestibular organs but also evokes responses from proprioception (Day & Fitzpatrick, 2005). In system analysis of human motion control, the approach is to isolate each part of the system to investigate its function based on the input-output relationships. Galvanic vestibular stimulation (GVS) is a technique which facilitates isolated stimulation of the vestibular system applying small electric currents (~ 1 mA) to alter the vestibular information from the organs. As a result GVS evokes a sensation of motion and consequently elicits vestibular reflexes to counteract the perceived motion. Although it has no natural equivalent it has been shown that this type of stimulation has the same frequency modulating effect on the vestibular neurons as natural motion (Day & Fitzpatrick, 2005).

Previous studies have applied GVS to standing subjects and it was shown that GVS elicits coherent muscle responses in the lower limbs (Fitzpatrick *et al.*, 1996). Stochastic

stimulations were applied in a wide range of frequencies from 0 to 50 Hz (Dakin *et al.*, 2007; Dakin *et al.*, 2010) wherein observed motions were modulated with amplitude and frequency of the stimuli. Applying sinusoidal currents, different components of muscle responses and their interactions with additional elements in the control loop have been investigated (Dakin *et al.*, 2011). Additionally, nonlinearities in the system have been explored (Day *et al.*, 2010) as well as the effect of adaptation to the stimulus on the sway response (Johansson *et al.*, 1995; Balter *et al.*, 2004b).

Although GVS has been used extensively in stance control studies, no efforts have been made to use this technique to shed light on remaining uncertainties regarding the vestibular contribution of the head-neck stabilization. The goal of this study was to determine whether GVS could be used as a method to investigate the role of the vestibular system in the control of head stabilization in seated subjects using GVS. We tested three hypotheses: (1) GVS evokes coherent motions in head and neck, (2) the resulting responses originate exclusively from the stimulation of vestibular afferents and (3) the responses are modulated with frequency and not amplitude of GVS. Non-parametric system identification techniques were applied to evaluate the first hypothesis. The second was tested by comparison of the results from vestibular stimulation tests with results from non-vestibular (NV) stimulation tests. The third hypothesis was evaluated by applying single sinusoidal stimulations of varying frequency and amplitude, as well as a sum of sinusoids to evaluate their cumulative effect.

Methods

Subjects

Eleven healthy subjects (6 male) between the ages of 18 and 42 with no history of vestibular or neck disorders participated in this study. The testing procedure was explained to the participants and their written consent was obtained prior to experiments. The experimental protocol was in accordance with the Declaration of Helsinki and was approved by the Human Research Ethics Committee at the Delft University of Technology.

Apparatus

A custom made galvanic stimulator (Balter *et al.*, 2004a), was used to generate the stimuli which met medical electrical equipment safety standard for human use (IEC-60601-1 (Medical electrical equipment – Part 1: General requirements for basic safety and essential performance)). The stimulator was current controlled ensuring that the same stimulation was applied to each subject regardless of their skin impedance. The input analog signal to the stimulator was generated using a DA board. The input current to and the output current from the stimulator were recorded with an analog board (Qualisys, Gothenburg, Sweden).

The vestibular stimulation was applied using carbon rubber electrodes (3.8 cm × 4.4 cm) coated with Spectra 360 electrode gel (Parker Laboratories, Fairfield, NJ). Electrodes were fixed in place using a swimming cap and/or adhesive tape. Two configurations were used: bipolar binaural and non vestibular (NV). The bipolar binaural configuration was chosen because it generates stronger responses and results in higher coherences compared to

monopolar configurations (Pavlik *et al.*, 1999; Scinicariello *et al.*, 2002). In the binaural configuration electrodes were placed on the mastoid processes. In the NV configuration one electrode was placed on the forehead and the other one on the seventh cervical vertebra (C7). This configuration was applied since it was a successful choice in revealing the vestibular origin of responses in stance control (Dakin *et al.*, 2007).

A motion capture system (Qualisys, Gothenburg, Sweden) was used to record kinematics. Six infra-red cameras (Oqus) captured all motions using reflective passive markers attached to subjects. The head motion was recorded using five markers, four attached to the helmet and one directly on the head close to trignon. The positions of these markers together with the head breadth were used to define the head as a rigid body with a local coordinate system at the estimated centre of gravity (Yoganandan *et al.*, 2009) oriented along the Frankfurt plane. Figure 1 shows the local coordinate system and the directions of translation and rotation used to measure the 6 degrees of freedom motion (rotations and translations). Looking in the direction of the axes, positive roll and pitch are defined clockwise and positive yaw is defined counterclockwise. In this coordinate system if the negative (cathodal) and positive (anodal) currents are placed on the right and left mastoids respectively the observed response will be negative roll and yaw towards the anode (left side) (Fitzpatrick & Day, 2004). Accordingly a change of polarity will result in positive roll and yaw towards the cathode (right side).

Torso motion was recorded using three markers attached to the sternum and T1 which were used to define the local coordinate system which was placed on the T1. The motion of torso was compared to the responses recorded in the natural sway tests (i.e. no stimulation, see [Protocol](#)) for all stimulation conditions confirming the assumption that the torso was confined by the seat belts.

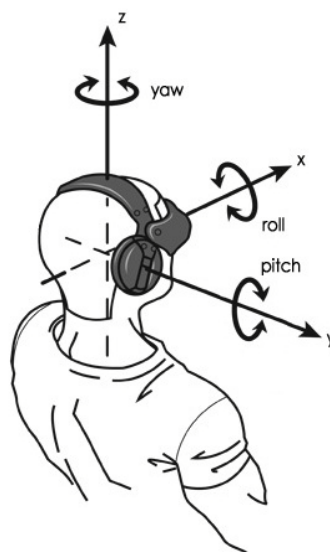


Figure 1. Roll, pitch, yaw and the direction of local coordinate system

Stimuli

Seven different stimuli (six single sinusoids and one multisine) were generated and applied in the binaural configuration. Table 1 lists the stimuli and their specifications. In the NV configuration three stimuli were applied: the multisine, sinusoid 3 (2 mA-0.4 Hz) and sinusoid 5 (2 mA-2 Hz).

Stimulus	Amplitude (mA)	Frequency (Hz)	Duration (sec)	No. of repetition
Sinusoid 1	0.5	1.2	80	2
Sinusoid 2	1	1.2	80	2
Sinusoid 3	2	0.4	80	2
Sinusoid 4	2	1.2	80	2
Sinusoid 5	2	2	80	2
Sinusoid 6	2	5.2	80	2
Multisine	2	0.4, 1.2, 2, 5.2	80	2

Table 1. Designed stimuli, corresponding amplitudes, frequencies and durations. The first six stimuli were single sines and the last one was a multisine.

Single sinusoids were chosen as stimulation signals for several reasons. First, sinusoids (and multisines) ensure the comfort of subjects and the absence of the extr vestibular cue on the cutaneous receptors commonly observed in pulse trains stimuli (Latt *et al.*, 2003). Second, periodic perturbations are deterministic excitations and as a result prevent spectral leakage which is an advantage over the white noise stimuli (Pintelon & Schoukens, 2001). Finally, since this study was the first attempt to explore the head and neck responses to GVS, this simple form of sinusoidal signals was used.

A multisine¹ was used to excite the system at several frequencies simultaneously. This was to eliminate the possibility of anticipation in human subjects. Furthermore, we can place an exact value of power at any desired frequency, increasing the signal to noise ratio (SNR).

For both excitation signals (single sine and multisine) frequency and amplitude were considered as perturbation signal design parameters. Previous studies on stance control reported high coherences (0.6-0.8 with PRBS and 0.5-0.6 with stochastic), in the ranges of 1–5 Hz (Johansson *et al.*, 1995) and 1–2 Hz (Pavlik *et al.*, 1999). Knowing the natural frequency of the head and neck system to be between 2 and 2.5 Hz (Tangorra *et al.*, 2003) the frequencies explored were selected from the range of 0 – 6 Hz, where it was expected that the majority of the system dynamics could be observed. Amplitudes of 0.5 – 2 mA (peak to peak) were chosen based on observation of movement in previous stance control studies (Pavlik *et al.*, 1999; Latt *et al.*, 2003; Dakin *et al.*, 2007). Additionally, amplitudes higher than 3 mA could cause pain or discomfort in subjects. To explore possible adaptation in responses to stimuli for the binaural configuration, each condition was repeated twice.

To reduce the experiment time and prevent fatigue the effects of frequency were explored using single sines at 2 mA and the effects of amplitude were explored using single sines at 1.2 Hz. 2 mA was chosen to maximize SNR and minimize subject discomfort (established during pilot study) and 1.2 Hz was chosen to ensure high coherence as observed in the literature (Pavlik *et al.*, 1999). The frequencies chosen for the single sines mimicked those

¹ The data in multisine tests is available for 8 subjects only.

used for the multisine, which was designed to have four frequencies (0.4, 1.2, 2.0 and 5.2 Hz). To check for the additivity (superposition) principle the power at each frequency in the multisine should be equal to the power of the single sine with the corresponding frequency. To achieve this, the multisine amplitude should have been ~ 3.5 mA to contain the same power per frequency as 2 mA single sines. This amplitude surpassed the limit of comfort for some subjects and as a result was discarded from the experiments. The multisine was therefore applied with the same amplitude as the single sines (2 mA), dividing the power over four frequencies. This was effectively equivalent to single sine perturbations of ~ 0.85 mA.

Protocol

Subjects sat on a chair fixed to the ground and were asked to maintain their head in the upright position while staying relaxed during the tests. A horizontal seatbelt across the chest was used to prevent the motion of torso and confine the responses solely to head and neck. During the tests subjects were blindfolded to exclude the visual input and were asked to listen to a science podcast (Quirks & Quarks²) to distract them from the stimulus.

According to previous studies with GVS on stance control a stimulus of longer than 60 seconds is sufficient to reveal the characteristics of the human response (Pavlik *et al.*, 1999). Therefore, the stimuli were applied twice each for 80 seconds. The experimental procedure in the binaural configuration consisted of sixteen trials. The six single sinusoids were performed first in a randomized order followed by the multisine tests. Additionally, natural head sway (NHS) tests (i.e. no stimulation) were performed before and after all stimulations as a control condition. The NV configuration was applied on only two subjects and performed after all aforementioned test conditions.

Analysis

To analyze the responses system identification techniques were used to establish the relationship between the head sway and stimulation. Calculated parameters and processing steps are discussed in this section. To interpret these results, a simplified model of the head and neck as a feedback control system is illustrated in Figure 2. The figure depicts the vestibular, proprioceptive and visual sensory system providing integrated information through a delay to the neural controller. Since subjects are blindfolded, the CNS can only rely on the information from proprioception and vestibular system to stabilize the head and neck.

Data processing

The two realizations of each stimulus were concatenated to form a signal of 160 seconds. This signal was divided into 32 segments of 5 seconds and averaged in both time and frequency domains. In the frequency domain this provided resolution of 0.2 Hz. The head rotation and translations calculated with the motion capture system showed considerable drift³. This trend (drift) did not follow any pattern and was of no interest for the analysis. To isolate the periodic component of the responses, each segment was detrended using the standard Matlab function. All calculations are performed using a custom Matlab code.

² <http://www.cbc.ca/quirks/>

³ The low frequency component of the data as opposed to the periodic component.

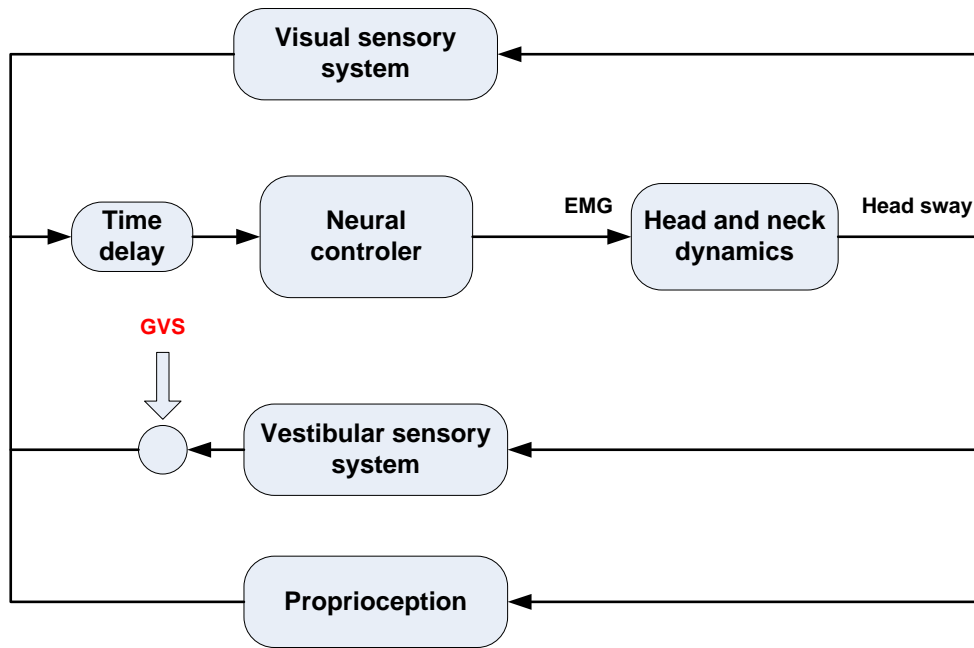


Figure 2. Head and neck feedback control. The information from proprioception, visual and vestibular sensory systems integrate to central nervous system and motor control commands are generated and then sent to the neck through afferent pathways. GVS signal alters the information in vestibular pathways to the CNS.

Non-parametric system identification

Various power spectra were calculated and averaged over the 32 segments (D) according to:

$$\hat{S}_{xy}(f) = \frac{1}{DN_d} \sum_{d=1}^D X_d^*(f) Y_d(f) \quad (1)$$

$$\hat{S}_{yy}(f) = \frac{1}{DN_d} \sum_{d=1}^D Y_d^*(f) Y_d(f) \quad (2)$$

Where $Y_d(f)$ and $X_d(f)$ are the fast fourier transforms of one segment of the output motion and input stimulation respectively, f is the frequency vector and $*$ represents the complex conjugate (Oppenheim *et al.*, 1999). The auto-spectral densities (Eq (2)) of the output signals were used to perform the comprehensive analysis of frequency and amplitude effects. This approach was chosen as the autospectral densities are specific to the output signal only. Both the cross and auto-spectral densities were used to calculate the frequency responses functions and coherence, both of which were also used in the analysis.

Frequency response functions (FRFs) of a LTI system provide a measure of input-output relationship. The gains and phases of the FRFs provide information on magnitude and timing of the output relative to the input. They were calculated in this study as:

$$\hat{H}_{xy} = \frac{\hat{S}_{xy}}{\hat{S}_{xx}} \quad (3)$$

The coherence squared values provide a measure of system linearity. If there is no noise and the system is linear then coherence will be 1. In the presence of noise (uncorrelated to the input) coherence squared represents the linear fraction of the response variance due to the input stimulus (Westwick & Kearney, 2003). The coherence squared values were calculated as:

$$\gamma_{xy}^2(f) = \frac{\left| \hat{S}_{xy}(f) \right|^2}{\hat{S}_{xx}(f) \cdot \hat{S}_{yy}(f)} \quad (4)$$

Assessing the level of significance for coherence was accomplished by establishing a significance limit according to:

$$C_{\alpha} = \frac{F_{2,2L-2}(\alpha)}{L-1 + F_{2,2L-2}(\alpha)} \quad (5)$$

Where L is the number of segments (32) for averaging, α is the type I error of 0.05 ($1-\alpha=0.95$) and F is the inverse of F-distribution⁴ with degrees of freedom 2 and 2L-2 (Shumway & Stoffer, 2010). If the values of coherences are greater than C_{α} then we can reject the null hypothesis which states the true coherence between the input and the output is zero ($\gamma_{xy}^2 = 0$).

It should be noticed that values for gain and phase of transfer function are only meaningful when there is significant coherence. As a result the calculation of these values on the non significant points should be avoided. Since different stimuli and several conditions were used in this study the exclusion of non significant points from transfer functions was not always practical. The data presented should be reviewed considering this matter.

Statistics

A repeated measures ANOVA was used to assess the effects of perturbation design parameters on the responses. Three separate ANOVA tests were performed across time segments, frequencies and amplitudes as independent variables (IVs) and their effect on the response amplitude, gain, phase and coherence of the system as dependent variables (DV) were investigated. A significance of 0.05 was used for all analyses.

In order to meet the assumptions of ANOVA (normality and homogeneity), the autospectral power and gain were log transformed. This reduced the deviations from the normal distribution (Gamst *et al.*, 2008). Since the results of ANOVA showed violation of homogeneity assumption we used Greenhouse-Geisser and Huynh-Feldt corrections to

⁴ The distribution of null hypothesis

account for this issue as these two estimates do not put the assumption of homogeneity on the data. Since Greenhouse-Geisser underestimates and Huynh-Feldt overestimates sphericity⁵, the p-values were calculated as average of the result of both adjustments.

Finally, a paired t-Test was performed to determine the effect of repeating each stimulus. Any adaptation to the stimulus should be revealed as a significant difference between the two repetitions. Detailed results of all statistical analyses can be found in [Appendix A](#).

Results

Response effects due to time

Figure 3 plots the roll and Y direction (mediolateral) translation response of a typical subject over a 5 second segment. These responses are the average of the 32 segments for each of the three amplitudes at a frequency of 1.2 Hz. For both rotation and translation obvious periodic motion can be observed for 1 and 2 mA at 1.2 Hz, while no obvious periodic motion can be seen at 0.5 mA. However, it is noted that 8 of 11 subjects demonstrated obvious periodic motion at all amplitudes.

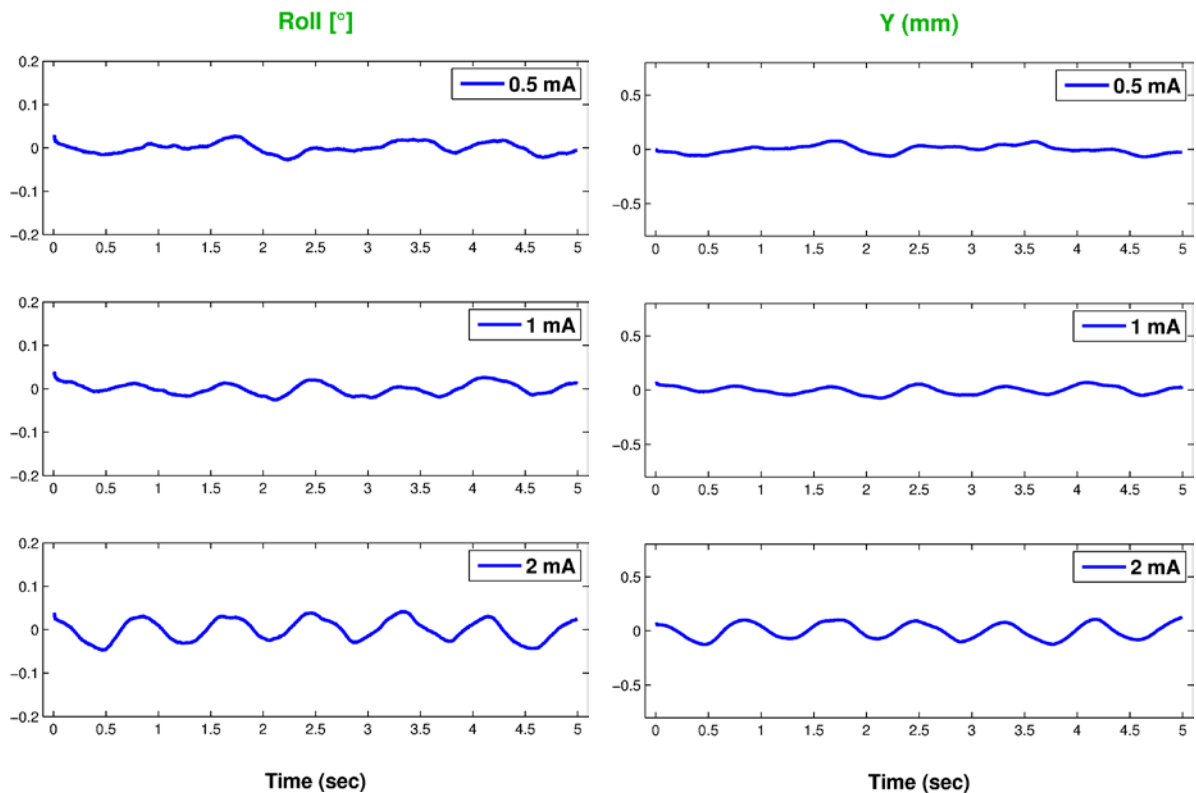


Figure 3. Motions in roll (left) and Y (right) directions averaged over 32 segments of 5 seconds (two realizations) for three different amplitudes of 0.5, 1 and 2 mA with frequency of 1.2 Hz. Data is for subject No. 4.

Although averaging in time revealed the periodic components of responses in some tests, the variations across different time segments is not clear. To assess the variance of the system across time auto-spectral density of the roll and Y translation of all 32 segments were

⁵ *Sphericity*: the variances of the differences between all pairs of the repeated measurements are equal.

examined. Figure 4 and Figure 5 show the spectral densities in roll and Y-translation (mediolateral) as a function of segment order for a typical subject. The spectra are plotted for the stimulated frequency only. Visual inspection of the results indicates a non-stationary response in all tests; however, no consistent pattern of time effect was observed in different stimulations for any subject. Furthermore, the effect of time evaluated across all subjects was not significant for all conditions with the exception of the 2 mA-2 Hz condition ($P < 0.01$) where the power in first four segments were higher than the rest of segments (by factor of 2.3 in rotation and 3.8 in translation). Further analysis of the 2 mA-2 Hz condition revealed that when removing the first four segments the effect of time was no longer significant. Therefore, these segments were removed from further analysis in the 2 mA-2 Hz condition and considered as a transient effect unimportant to the steady state nature observed thereafter. The origin of this transient effect for only this condition however could not be explained.

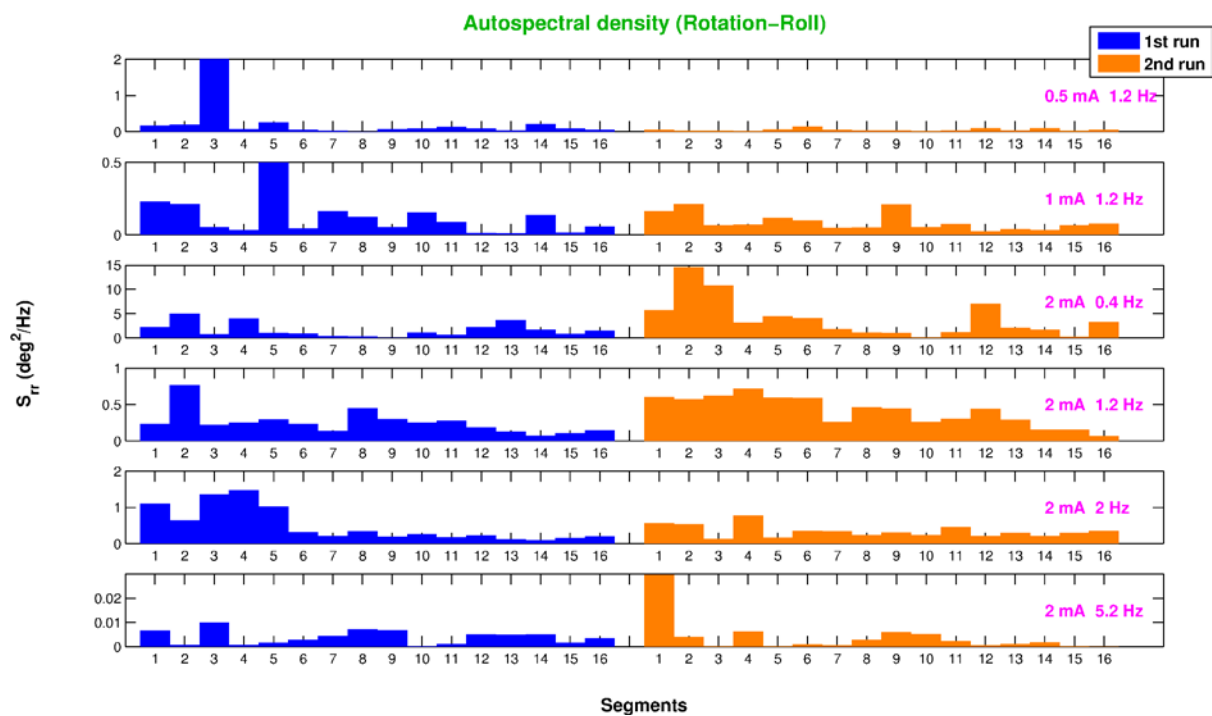


Figure 4. Autospectral density of response at the stimulated frequency in roll over 32 segments in time. The blue and orange segments are from the first and second realizations of each stimulus respectively. The scale of each subplot is different for presentation matters. Data is for subject No. 4.

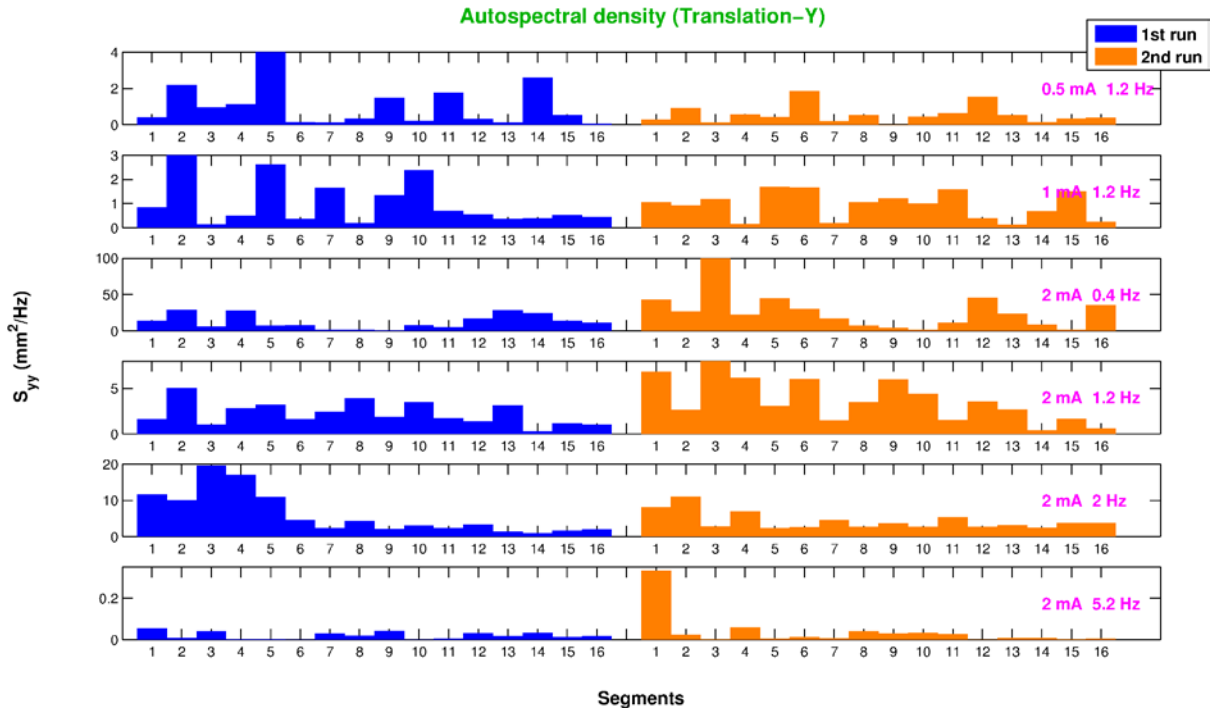


Figure 5. Autospectral density of response at the stimulated frequency in Y direction over 32 segments in time. The blue and orange segments are from the first and second realizations of each stimulus respectively. The scale of each subplot is different for presentation matters. Data is for subject No. 4.

Responses in frequency domain

Auto-spectral densities

Having satisfied the assumption of stationarity, the autospectral densities were averaged over 32 segments. Figure 6 shows the autospectral densities of the separate stimuli, wherein significant power can be observed at the stimulated frequency. Although spectral power can also be observed at the harmonics of each stimuli, this was substantially smaller (1000 times) than that of the stimulated frequency and considered negligible. The origin of this problem was believed to be due to a technical error when generating the output stimuli; however this could not be confirmed.

Figure 7 shows the autospectral densities of responses in roll-pitch-yaw and XYZ directions of a typical subject for all frequencies tested at 2 mA. All individual subject responses can be found in [Appendix B](#). It is observed that the output shows dominant power at the stimulated frequencies of 1.2 and 2 Hz, particularly for roll, yaw and y-translation. At 5.2 Hz low power is observed which could be due to higher noise level and mechanical filtration due to inertia at high frequencies, and at 0.4 Hz the power is similar to the noise measured at the adjacent frequencies. Although the power at these two points was low, the coherence values and averages over all subjects should be reviewed to make conclusions about the behavior of the system at stimulated frequencies. Similar responses were observed for both the 0.5 and 1.0 mA results at 1.2 Hz.

Substantial power was observed across the entire bandwidth in pitch and X-translation which was attributed to breathing producing a form of noise specific to these signals. Higher power was observed in roll compared to the yaw component and in the Y-direction translation

Transfer functions and coherences

Figure 8 shows gain, phase and coherence of the system in rotation and translation of a typical subject for both single sines and multisines at an amplitude of 2 mA. In these figures the results of single sine stimuli are shown with empty circles and the multisine is plotted with connected squares at the same four frequency points. Only the roll, yaw and Y-translation responses were plotted here as the pitch, X-translation and Z-translation were insignificant at almost every point for every subject. All responses can be found in [Appendix B](#).

Examining the rotation response first, an increase in the stimulation frequency results in a significant decrease ($P < 0.001$) of gain. Consistent with the reported effect of GVS in the literature (see [Discussion](#)), the gain for roll was significantly higher at all frequency points ($P < 0.001$ for 0.4 Hz, $P < 0.05$ for 1.2 Hz and $P < 0.01$ for 2 Hz) with the exception of 5.2 Hz where the gain for yaw was significantly higher ($P < 0.01$). This higher frequency yaw response was attributed to the lower rotational inertia in yaw (Yoganandan *et al.*, 2009) when compared to pitch or roll. In the phase plot a significantly increasing ($P < 0.001$) lag was observed as the stimulation frequency increased. At the lowest frequency the phase was 90 degrees and degraded toward -180 at the highest frequency. This was consistent with the gain behavior and the effect of inertial forces as a function of frequency. Coherence in rotation was always significant for the roll and yaw components. Frequency had a significant effect on the coherences for the roll with reduced coherences at 5.2 Hz ($P < 0.001$). The observed changes in the yaw component across frequencies were not significant but the P-values were in the marginal interval ($0.05 < P < 0.06$).

Translational response components show similar behavior as those observed in rotation, where the Y-direction response matched the roll and yaw responses. Gain and phase decreased significantly ($P < 0.001$) with increasing frequency. The coherence in Y-direction was significant in all cases and was larger than the two other directions. Finally, frequency had a significant effect ($P < 0.001$) on Y-direction coherence, which was high in all points with the exception of 5.2 Hz.

Figure 9 shows the FRFs and coherences of all amplitudes at 1.2 Hz of a typical subject. Although the responses for this particular subject show a decreasing gain and increasing phase with increasing amplitude, no significant effect could be attributed to the group response for either gain or phase. Increasing stimulation amplitude had a significant increasing effect (roll: $P < 0.05$, yaw: $P < 0.001$, Y: $P < 0.01$) on coherence. This can be attributed to a direct increase in SNR with an increase in stimulation intensity.

For completion, Figure 10 and Figure 11 plot the group average responses (mean and std) for the single sine and multisine conditions respectively. The same patterns described for the individual subject can be seen in the group average. Furthermore, substantial variance can be seen by the large standard deviations which reflected the high between subject variability.

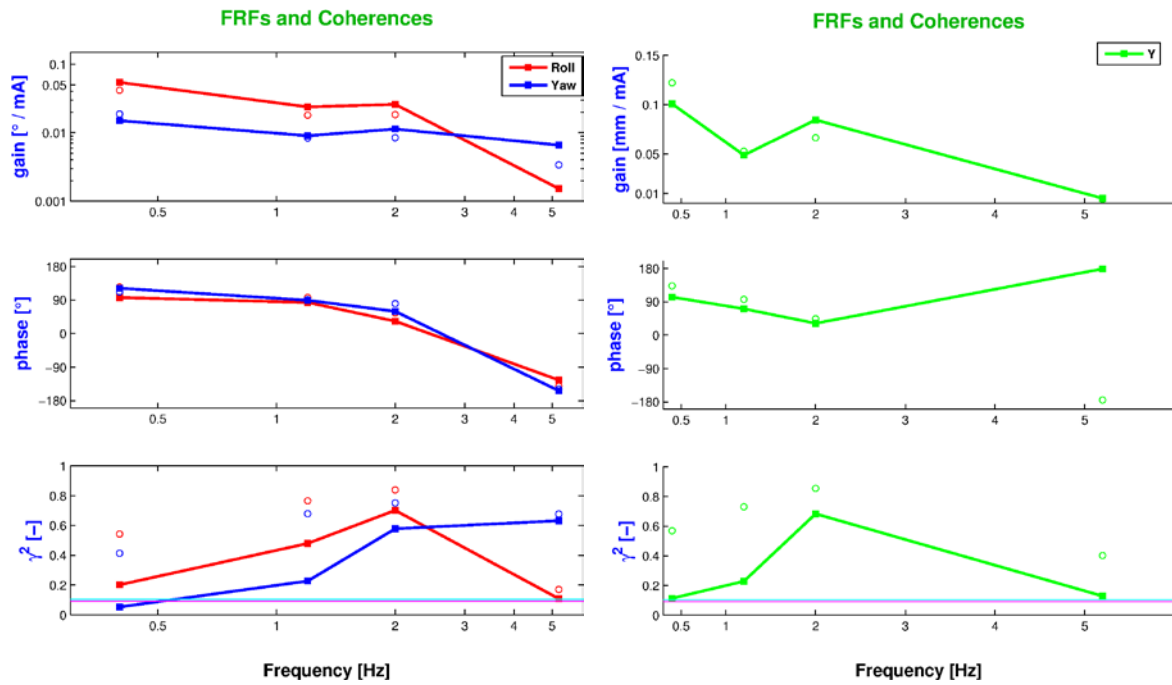


Figure 8. FRFs and coherences of rotations (left) and translations (right) for 2 mA stimuli. Single sines vs. Multisine across four frequencies. Data is for subject No. 4.

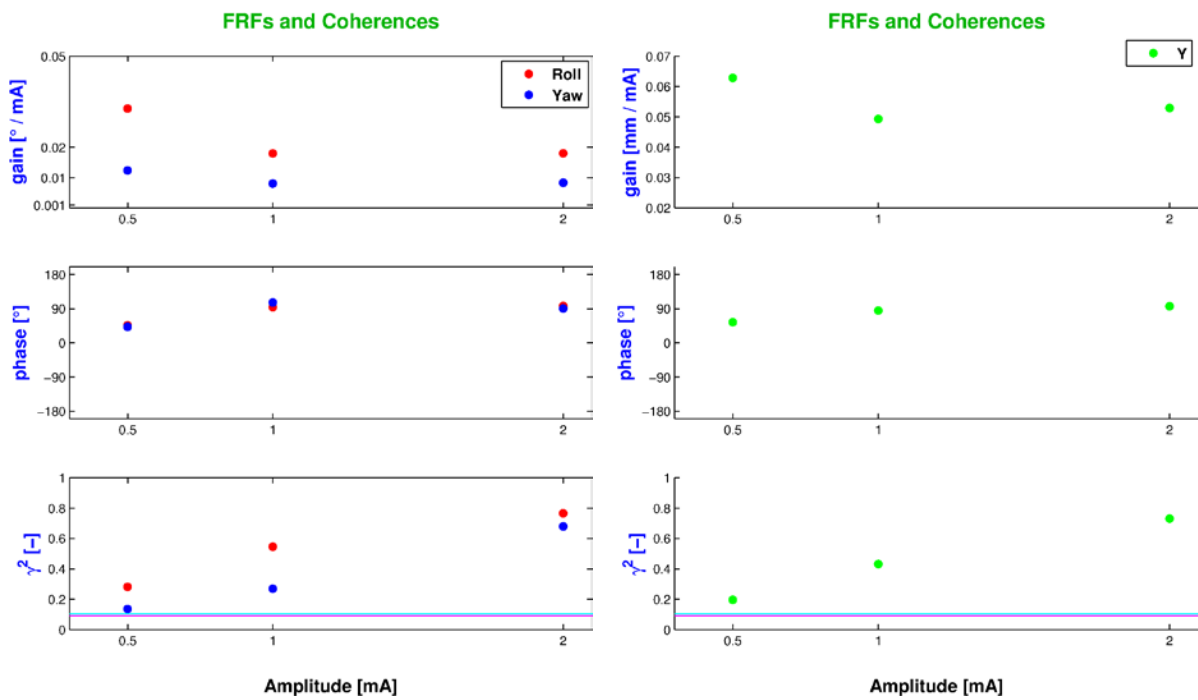


Figure 9. FRFs and coherences of rotations (left) and translations (right) for 1.2 Hz stimuli in three amplitudes. Data is for subject No. 4.

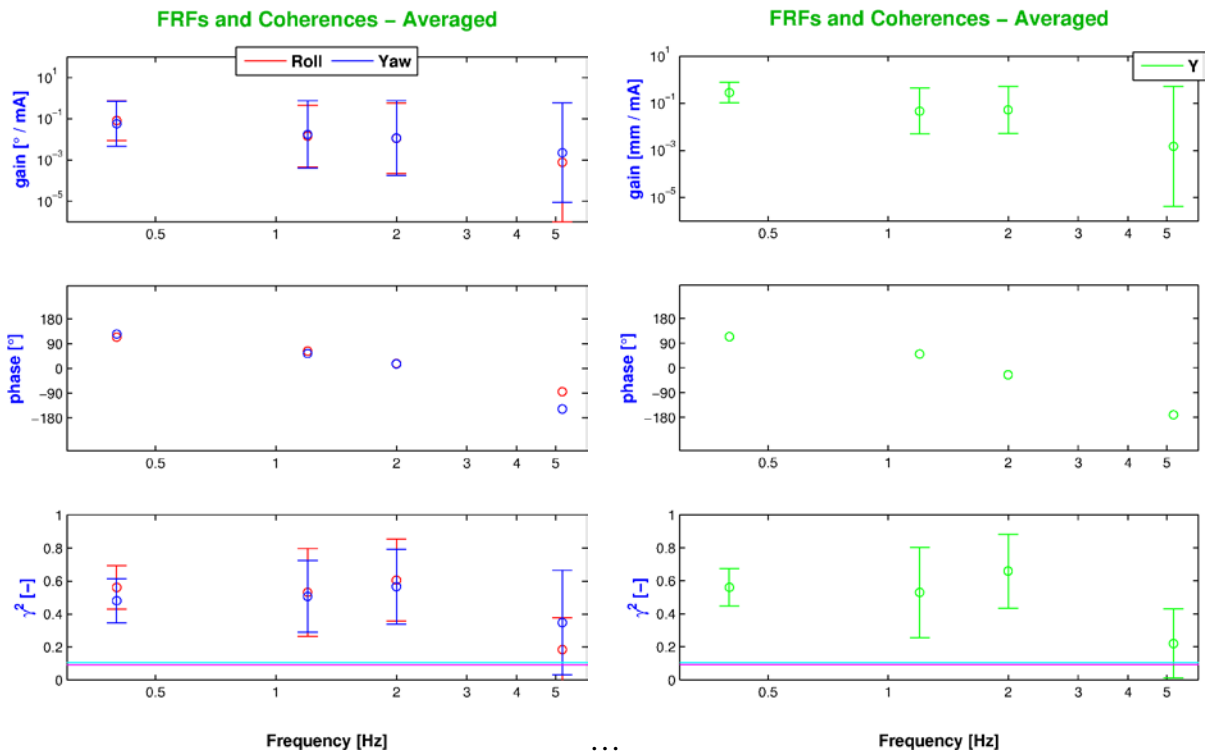


Figure 10. FRFs and coherences averaged (mean \pm SD) over 11 subjects for single sine stimuli. The rotation components are shown at left and translations at right.

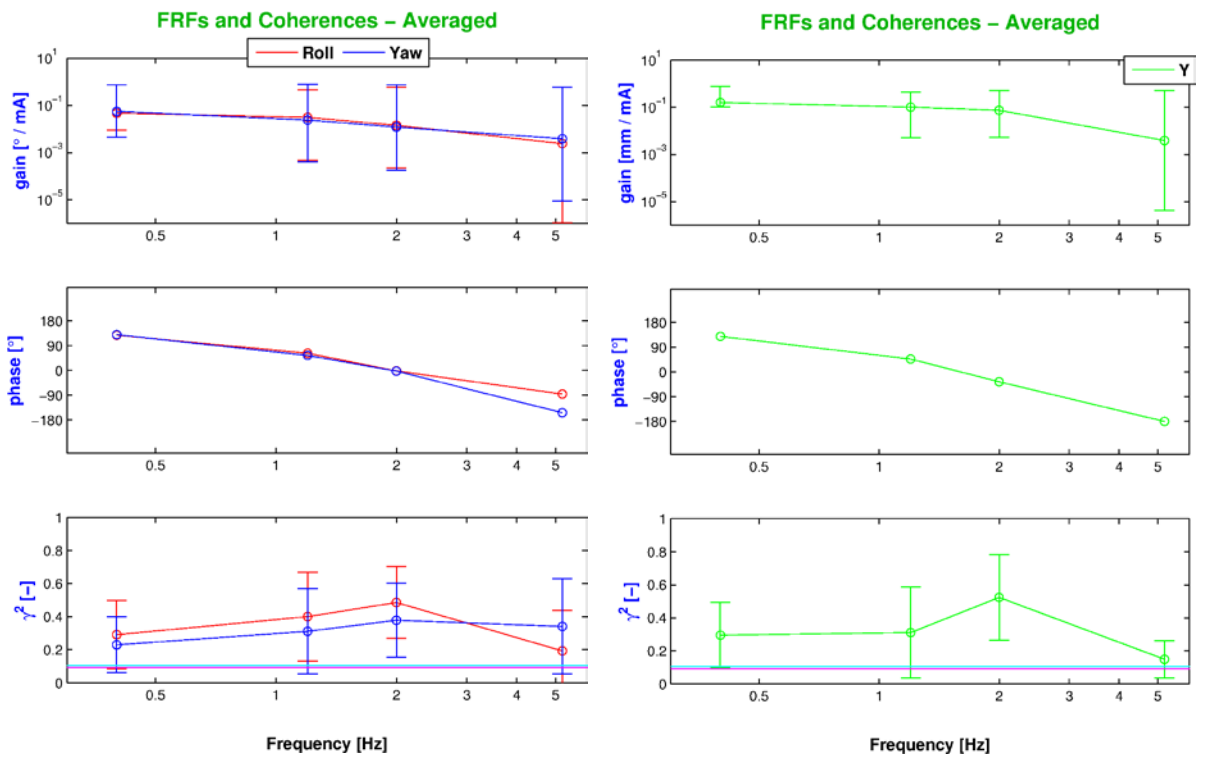


Figure 11. FRFs and coherences averaged (mean \pm SD) over 8 subjects for multisine stimuli. The rotation components are shown at left and translations at right.

Multisine vs. single sine

Responses observed in multisine stimulations were similar to those from single sines. The gain and phase decrease with frequency. Roll and yaw and Y-translation components always showed significant coherence. However, multisine responses exhibited lower coherences, most likely due to the fact that multisines results in division of power over multiple frequencies and lower SNR. Comparing the single sines and multisines stimulations, no significant difference could be found for gain at all frequency points.

Non-vestibular stimulation

To evaluate the hypothesis that the coherent responses evoked by GVS originate from vestibular afferents and not cutaneous cues the results from the non-vestibular configuration were examined. The coherences of the responses are shown in Figure 12 for rotations and translations. The coherences were non-significant for both the single sines (0.4 and 2 Hz) and the multisine. This indicates that the coherent motion observed in this study originates from the stimulation of the vestibular organ.

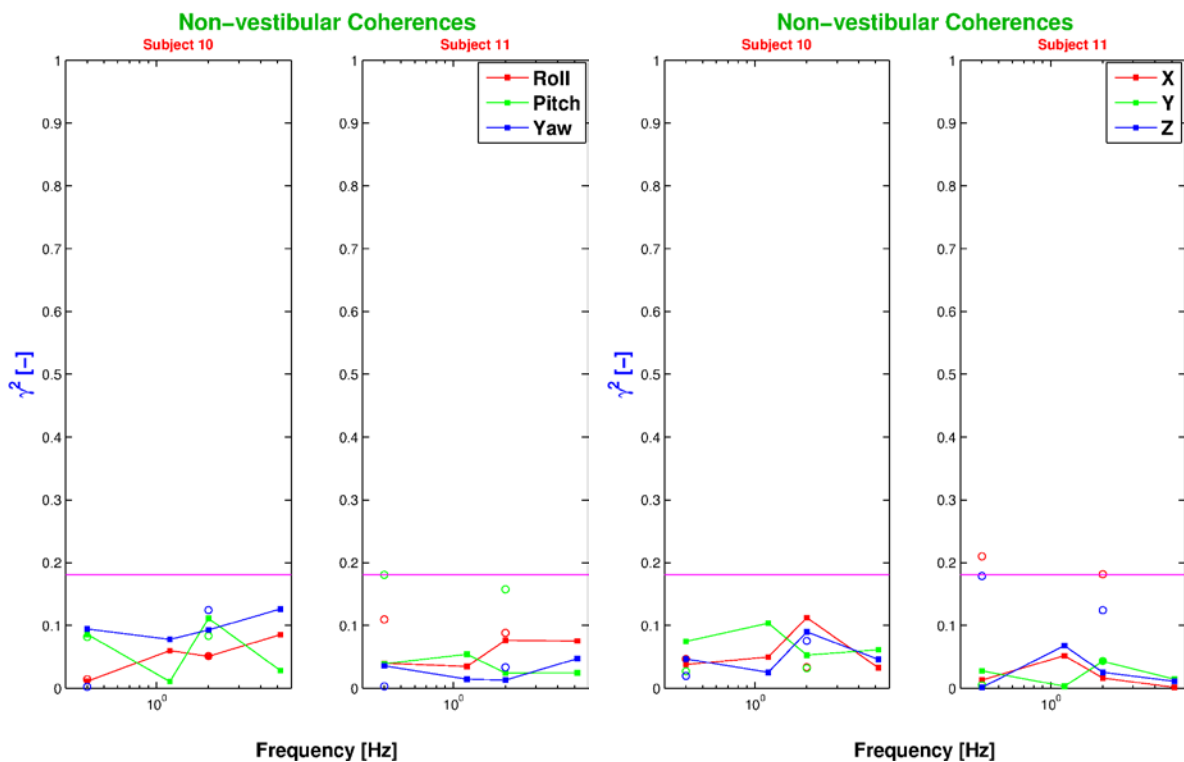


Figure 12. Coherences of rotations (first two plots from left) and translations (first two plots from right) for non-vestibular configuration. Left column presents the data for subject 10 and the right column for subject 11.

Discussion

The primary aim of this study was to determine whether galvanic vestibular stimulation could be used to identify the vestibular contribution of head-neck stabilization. We tested three hypotheses that (1) coherent motion is evoked in head and neck with GVS (2) the resultant motion is of a vestibular origin exclusively and (3) modulation of responses occurs across stimulation frequencies and amplitude.

Coherent motion

Bilateral bipolar galvanic vestibular stimulation is known to primarily affect the semicircular canals, inducing the sensation of roll and yaw rotation in the head. It has been observed in stance control that bipolar GVS results in lateral (Y-direction) sway motions. Vector summation of the separate canals responses suggest that the roll is larger in magnitude than the yaw (Fitzpatrick & Day, 2004). In this study, coherent head motion in roll, yaw and Y-translation was observed in both single sine and multisine stimulation conditions for all amplitude and frequencies considered. Although magnitude of observed motions was in the order of natural sway (0.1 mm and 0.1 deg), the responses were changing coherently with the stimuli (single sines and multisines). The high accuracy of the motion capture system (± 0.01 mm) made this possible.

The directionality of the responses suggests the origin of the movement to be of a vestibular nature in reaction to the electrical stimulation and not possible cutaneous cues (i.e. via electrodes being placed left and right). This was further confirmed via the non-vestibular stimulation conditions, where electrodes were placed on the forehead and (C7). The lack of coherent motion in any of the observed directions during this condition supports the claim.

Response characteristics

The frequency response functions provide valuable information on the system behavior. In this study we were able to explore the system characteristics in the range of 0–6 Hz where observable kinematic responses occur. For both rotation and translation, modulation of gain and phase was observed with increasing frequency. The lowest frequency had a phase advance of ~ 90 degrees which decreased toward -180 at the highest frequency. The 90 degrees phase lead indicates differentiation action which is consistent to prior knowledge on semicircular canals; a damped second order system which act as velocity sensors (Vanbuskirk *et al.*, 1976; Obrist, 2007). Gain and phase plots of the responses (Figure 10 and Figure 11) resemble behavior of an overdamped second order system. This is consistent with previous findings suggesting head and neck is a quasi linear second order system (Viviani & Berthoz, 1975). As a result the head and neck dynamics (Figure 2) could be modeled as an inverted pendulum.

The coherence values were high at 0.4, 1.2 Hz and 2 Hz. The degradation of coherence at 5.2 Hz was attributed to the filtering inertial effects which minimized movement and caused low SNRs. The values obtained for coherences in this study were higher than those reported (~ 0.2) in stance control kinematics using stochastic stimuli (Fitzpatrick *et al.*, 1996).

The amplitude exploration showed no significant modulation of gain and phase with an increase in the magnitude of the input. This indicates the linear characteristics of the system i.e. two fold increase of input results in two fold increase of output. In contrast, coherence values significantly increased with amplitude up to as high as 0.8 during the 2 mA stimulations. This indicates the presence of strong SNR at 2 mA of the input, which decreased with decreasing amplitude. This suggests that coherences being less than 1 were the result of the noise in the system and not a nonlinear behavior. In addition to this, the mechanics of the vestibular system are established as being linear in the range of frequencies from 0.01 Hz to 30 Hz (Bronzino, 2000). This shows the validity of our assumption to consider the system as LTI. Although the application of stronger stimuli would improve SNR and further show linearity, it was omitted due to the pain and discomfort in some subjects.

A new finding of this study is the effect of sinusoidal currents on GVS response from head-neck system. Previously single sinusoids were applied to stance control (Latt *et al.*, 2003) and revealed some characteristics of the system. However a frequency response analysis was not performed and no information was available on the coherence of responses. We demonstrated that sinusoidal currents could elicit highly coherent responses in head-neck system. Additionally, this study demonstrates that multisine signals can similarly reveal the characteristics of the system and achieve significant coherence values. Although the power density of multisines was lower than the amplitude equivalent single sines the coherence values were as high as 0.7. This value is higher than what previously reported using filtered white noise. Another advantage of multisines is the unpredictable nature they have to human subjects. This property is important to exclude non-reflexive components from the response. The significant coherences in multisine stimulations suggest that the responses were of a reflexive origin. Considering the single sine results matched those of the multisines it is reasonable to assume those responses as being of a reflexive nature responding to vestibular stimulation.

Subject variability and reliability

The observed responses of the head and neck to GVS showed substantial variability between subjects. This has been observed in previous research with GVS, where its effect on eye movement was evaluated (MacDougall *et al.*, 2002; MacDougall *et al.*, 2003). Those findings showed that individual differences in responses to GVS are similar to those from caloric stimulation. It was further argued that these types of vestibular stimulation are unnatural and as a result more variability in responses can be expected in humans. This was in contrast to more natural stimuli such as mechanical perturbations in which human subjects show similar responses (MacDougall *et al.*, 2002). Therefore, the variability across subjects observed here was considered inherent to GVS characteristics and not related to experimental design.

Considering large between subjects variability, previous GVS studies have evaluated the reliability of their findings by showing that the responses are reproducible within each subject (MacDougall *et al.*, 2002; MacDougall *et al.*, 2003). To account for this matter in our study we repeated each stimulus once and compared the two responses for each subject using a paired t-test (two tailed). No significant effect of repetition on the output power was observed for any stimulation condition.

Limitations

The current measured data from the vestibular responses includes the effect of feedback loops (vestibular and proprioceptive). To remove the effect of feedback (i.e. open the loop) we need to measure at different locations in the loop and apply the joint input-output method to mathematically cancel the effect of feedback. This is important since we are interested in the characteristics of the vestibular sensory system per se. It is possible to achieve this by measuring EMG activity. An added benefit to EMG measurements is that one can bypass mechanical filtration and explore system behavior over a wider bandwidth of frequencies. In an attempt to do so in this study, surface EMG measurements were performed on two subjects. Large artifacts were induced by GVS in the EMG signals which were removed by simple filtering methods. However after artifact removal no significant effects of the stimuli could be found in the sEMG. This issue is discussed further in [Appendix C](#).

Another limitation in this study was the inability to separate the cervicocollic reflexes from vestibulocollic ones. Galvanic stimulation as a standalone perturbation cannot differentiate between these two types of responses.

Conclusions

Four conclusions can be inferred from the results of this research:

- Galvanic vestibular stimulation results in coherent motions in the head and neck similar to the responses observed in stance control studies.
- The evoked coherent motions are exclusively the result of vestibular afferents stimulated by electric current. This could be only achieved by applying the stimulus over the mastoid processes.
- Frequency and stimulus type can be used as design parameters to modulate the vestibular responses and explore the behavior of the system efficiently.
- The choice of amplitude has a significant effect on the SNR and coherences which is important in revealing linear characteristics of the system and eliciting observable responses.

Future work

An important unanswered question in this study was the role of each component in the system on the output response. Due to the aforementioned limitations the solution to this problem could not be implemented. A successful measurement of muscle activities, which may be possible via indwelling EMG, would help differentiate between the vestibular reflexes and the system mechanics. Separation of VCR and CCR in the head-neck stabilization control, may be achieved through the combination of mechanical perturbations and GVS. One possible obstacle in applying this approach is the difference in the order of magnitude of responses for two perturbation types. A mechanical perturbation on a 6 DOF platform produces head and neck motions in the order 1 cm while GVS results in motions of the order 0.1 mm. As a result the large amplitude of the mechanical perturbation may result in dominance of the proprioception information (Figure 2), causing the CNS to ignore the

galvanically evoked vestibular information. Further investigation is needed on this matter to approve feasibility of this approach.

References

- Balter SGT, Stokroos RJ, De Jong I, Boumans R, Van de Laar M & Kingma H. (2004a). Background on methods of stimulation in galvanic-induced body sway in young healthy adults. *Acta Oto-Laryngologica* **124**, 262-271.
- Balter SGT, Stokroos RJ, Eterman RMA, Paredis SAB, Orbons J & Kingma H. (2004b). Habituation to galvanic vestibular stimulation. *Acta Oto-Laryngologica* **124**, 941-945.
- Bronzino JD. (2000). *The biomedical engineering handbook*. Springer.
- Dakin CJ, Inglis JT & Blouin JS. (2011). Short and medium latency muscle responses evoked by electrical vestibular stimulation are a composite of all stimulus frequencies. *Experimental Brain Research* **209**, 345-354.
- Dakin CJ, Luu BL, van den Doel K, Inglis JT & Blouin JS. (2010). Frequency-Specific Modulation of Vestibular-Evoked Sway Responses in Humans. *J Neurophysiol* **103**, 1048-1056.
- Dakin CJ, Son GML, Inglis JT & Blouin JS. (2007). Frequency response of human vestibular reflexes characterized by stochastic stimuli. *Journal of Physiology-London* **583**, 1117-1127.
- Day BL & Fitzpatrick RC. (2005). The vestibular system. *Current Biology* **15**, R583-R586-R583-R586.
- Day BL, Marsden JF, Ramsay E, Mian OS & Fitzpatrick RC. (2010). Non-linear vector summation of left and right vestibular signals for human balance. *Journal of Physiology-London* **588**, 671-682.
- Fitzpatrick R, Burke D & Gandevia SC. (1996). Loop gain of reflexes controlling human standing measured with the use of postural and vestibular disturbances. *J Neurophysiol* **76**, 3994-4008.
- Fitzpatrick RC & Day BL. (2004). Probing the human vestibular system with galvanic stimulation. *J Appl Physiol* **96**, 2301-2316.
- Gamst G, Meyers LS & Guarino AJ. (2008). *Analysis of variance designs: a conceptual and computational approach with SPSS and SAS*. Cambridge University Press.

- Johansson R, Magnusson M & Fransson PA. (1995). GALVANIC VESTIBULAR STIMULATION FOR ANALYSIS OF POSTURAL ADAPTATION AND STABILITY. *IEEE Trans Biomed Eng* **42**, 282-292.
- Keshner EA, Cromwell RL & Peterson BW. (1995). MECHANISMS CONTROLLING HUMAN HEAD STABILIZATION .2. HEAD-NECK CHARACTERISTICS DURING RANDOM ROTATIONS IN THE VERTICAL PLANE. *J Neurophysiol* **73**, 2302-2312.
- Keshner EA & Peterson BW. (1995). MECHANISMS CONTROLLING HUMAN HEAD STABILIZATION .1. HEAD-NECK DYNAMICS DURING RANDOM ROTATIONS IN THE HORIZONTAL PLANE. *J Neurophysiol* **73**, 2293-2301.
- Latt LD, Sparto PJ, Furman JM & Redfern MS. (2003). The steady-state postural response to continuous sinusoidal galvanic vestibular stimulation. *Gait & Posture* **18**, 64-72.
- MacDougall HG, Brizuela AE, Burgess AM & Curthoys IS. (2002). Between-subject variability and within-subject reliability of the human eye-movement response to bilateral galvanic (DC) vestibular stimulation. *Experimental Brain Research Experimentelle Hirnforschung Expérimentation Cérébrale* **144**, 69-78.
- MacDougall HG, Brizuela AE & Curthoys IS. (2003). Linearity, symmetry and additivity of the human eye-movement response to maintained unilateral and bilateral surface galvanic (DC) vestibular stimulation. *Experimental Brain Research Experimentelle Hirnforschung Expérimentation Cérébrale* **148**, 166-175.
- Obrist D. (2007). Fluidmechanics of semicircular canals – revisited. *Zeitschrift für angewandte Mathematik und Physik* **59**, 475-497.
- Oppenheim AV, Schafer RW & Buck JR. (1999). *Discrete-Time Signal Processing (2nd Edition)*. Prentice Hall.
- Pavlik AE, Inglis JT, Lauk M, Oddsson L & Collins JJ. (1999). The effects of stochastic galvanic vestibular stimulation on human postural sway. *Experimental Brain Research* **124**, 273-280.
- Pintelon R & Schoukens J. (2001). *System Identification: A Frequency Domain Approach*. Wiley-IEEE Press.
- Purves D, Augustine GJ, Fitzpatrick D, Hall WC, Lamantia A-S, McNamara JO & Williams SM. (2008). *Neuroscience*. Sinauer Associates.

- Scinicariello AP, Inglis JT & Collins JJ. (2002). The effects of stochastic monopolar galvanic vestibular stimulation on human postural sway. *J Vestib Res-Equilib Orientat* **12**, 77-85.
- Shumway RH & Stoffer DS. (2010). *Time Series Analysis and Its Applications: With R Examples*. Springer.
- Tangorra JL, Jones LA & Hunter IW. (2003). Dynamics of the human head-neck system in the horizontal plane: joint properties with respect to a static torque. *Annals of Biomedical Engineering* **31**, 606-620.
- Vanbuskirk WC, Watts RG & Liu YK. (1976). FLUID-MECHANICS OF SEMICIRCULAR CANALS. *J Fluid Mech* **78**, 87-&.
- Viviani P & Berthoz A. (1975). Dynamics of the head-neck system in response to small perturbations: analysis and modeling in the frequency domain. *Biological Cybernetics* **19**, 19-37.
- Westwick DT & Kearney RE. (2003). *Identification of Nonlinear Physiological Systems*. Wiley-IEEE Press.
- Yoganandan N, Pintar FA, Zhang JY & Baisden JL. (2009). Physical properties of the human head: Mass, center of gravity and moment of inertia. *J Biomech* **42**, 1177-1192.

Appendices

- [Appendix A](#) – Statistical tables
Results of statistical tests in detail
- [Appendix B](#) – Analysis results for all subjects
Data presented in the paper for a typical subject is plotted here for 11 subjects' dataset
- [Appendix C](#) – EMG measurements and analysis
The results of EMG recordings and the outcome

Appendix A – Statistical tables

Statistical tables

	0.5 mA 1.2 Hz	1 mA 1.2 Hz	2 mA 0.4 Hz	2 mA 1.2 Hz	2 mA 2 Hz	2 mA 5.2 Hz
Roll (deg)	0.362	0.403	0.163	0.175	0.006, 0.134	0.211
Yaw (deg)	0.223	0.388	0.191	0.090	0.014, 0.168	0.271
Y (mm)	0.059	0.287	0.137	0.112	0.007, 0.071	0.093

Table A 1. P-values of ANOVA across time segments on autospectral powers for single sines on 11 subjects. The red values show the results across all segments for that test and the green values show the results with the first four segments removed.

	Single sines			Multisines		
	Roll	Yaw	Y	Roll	Yaw	Y
Sphericity Assumed	< 0.001	< 0.001	< 0.001	< 0.001	< 0.001	< 0.001
Greenhouse-Geisser	< 0.001	< 0.001	< 0.001	< 0.001	< 0.001	< 0.001
Huynh-Feldt	< 0.001	< 0.001	< 0.001	< 0.001	< 0.001	< 0.001

Table A 2. P-values of ANOVA for **autospectral powers in roll, yaw and Y direction** across four **frequencies**. The single sines are on 11 subjects and multisines on 8 subjects. An average of Greenhouse-Geisser and Huynh-feldt is considered as the P-value.

	Single sines		
	Roll	Yaw	Y
Sphericity Assumed	0.001	0.006	< 0.001
Greenhouse-Geisser	0.001	0.013	0.001
Huynh-Feldt	0.001	0.009	0.001

Table A 3. P-values of ANOVA for **autospectral powers in roll, yaw and Y direction** across three **amplitudes**. An average of Greenhouse-Geisser and Huynh-feldt is considered as the P-value.

	Single sines			Multisines		
	Roll	Yaw	Y	Roll	Yaw	Y
Sphericity Assumed	< 0.001	< 0.001	< 0.001	< 0.001	< 0.001	< 0.001
Greenhouse-Geisser	< 0.001	< 0.001	< 0.001	< 0.001	< 0.001	< 0.001
Huynh-Feldt	< 0.001	< 0.001	< 0.001	< 0.001	< 0.001	< 0.001

Table A 4. P-values of ANOVA for gains in roll, yaw and Y direction across four frequencies. The single sines are on 11 subjects and multisines on 8 subjects. An average of Greenhouse-Geisser and Huynh-feldt is considered as the P-value.

	Single sines		
	Roll	Yaw	Y
Sphericity Assumed	0.134	0.155	0.192
Greenhouse-Geisser	0.156	0.172	0.199
Huynh-Feldt	0.152	0.168	0.193

Table A 5. P-values of ANOVA for gains in roll, yaw and Y direction across three amplitudes. An average of Greenhouse-Geisser and Huynh-feldt is considered as the P-value.

Single sines			Multisines		
Roll	Yaw	Y	Roll	Yaw	Y
< 0.001	< 0.001	< 0.001	0.001	< 0.001	< 0.001

Table A 6. P-values of ANOVA for phases in roll, yaw and Y direction across four frequencies. The single sines are on 11 subjects and multisines on 8 subjects.

Single sines		
Roll	Yaw	Y
0.6957	0.8526	0.5909

Table A 7. P-values of ANOVA for phases in roll, yaw and Y direction across three amplitudes.

	Single sines			Multisines		
	Roll	Yaw	Y	Roll	Yaw	Y
Sphericity Assumed	< 0.001	0.042	< 0.001	0.006	0.393	0.003
Greenhouse-Geisser	< 0.001	0.067	< 0.001	0.012	0.386	0.006
Huynh-Feldt	< 0.001	0.052	< 0.001	0.006	0.393	0.003

Table A 8. P-values of ANOVA for **coherences in roll, yaw and Y direction** across four **frequencies**. The single sines are on 11 subjects and multisines on 8 subjects. An average of Greenhouse-Geisser and Huynh-feldt is considered as the P-value.

	Single sines		
	Roll	Yaw	Y
Sphericity Assumed	0.034	< 0.001	0.003
Greenhouse-Geisser	0.047	< 0.001	0.010
Huynh-Feldt	0.039	< 0.001	0.007

Table A 9. P-values of ANOVA for **coherences in roll, yaw and Y direction** across three **amplitudes**. An average of Greenhouse-Geisser and Huynh-feldt is considered as the P-value.

	Single sines	Multisines
	Roll vs. Yaw	Roll vs. Yaw
0.4 Hz	0.001	0.819
1.2 Hz	0.003	0.816
2 Hz	0.004	0.385
5.2 Hz	< 0.001	0.008

Table A 10. P-values of paired t-test between **autospectral powers of roll and yaw** in four frequencies. The single sines are on 11 subjects and multisines on 8 subjects.

	Single sines	Multisines
	Roll vs. Yaw	Roll vs. Yaw
0.4 Hz	< 0.001	0.397
1.2 Hz	0.024	0.175
2 Hz	0.004	0.068
5.2 Hz	0.006	0.010

Table A 11. P-values of paired t-test between **gains of roll and yaw** in four frequencies. The single sines are on 11 subjects and multisines on 8 subjects.

	Single sines	Multisines
	Roll vs. Yaw	Roll vs. Yaw
0.4 Hz	0.003	0.179
1.2 Hz	0.309	0.028
2 Hz	0.132	0.030
5.2 Hz	0.028	0.076

Table A 12. P-values of paired t-test between **coherences of roll and yaw** in four frequencies. The single sines are on 11 subjects and multisines on 8 subjects.

	Single sine vs. Multisine	
	Roll	Yaw
0.4 Hz	0.102	0.241
1.2 Hz	0.282	0.608
2 Hz	0.878	0.662
5.2 Hz	0.006	0.006

Table A 13. P-values of paired t-test between **single sines and multisines in roll and yaw** for four frequencies. The single sines are on 11 subjects and multisines on 8 subjects.

	Single sines		
	Roll	Yaw	Y
Sphericity Assumed	.462	0.657	0.420
Greenhouse-Geisser	.419	0.601	0.407
Huynh-Feldt	.438	0.657	0.420

Table A 14. P-values of ANOVA for gains in roll, yaw and Y direction across three amplitudes of single sines and multisine value at 1.2 Hz. An average of Greenhouse-Geisser and Huynh-feldt is considered as the P-value.

Stimulus	Sig. (2-tailed)
0.5 mA 1.2 Hz	.643
1 mA 1.2 Hz	.821
2 mA 0.4 Hz	.992
2 mA 1.2 Hz	.947
2 mA 2 Hz	.115
2 mA 5.2 Hz	.718

Table A 15. Paired t-test result for two different realizations of each single sine stimulus. The P-values for significance shows no effect of repetition.

Appendix B – Results for all subjects

Analysis results for all subjects

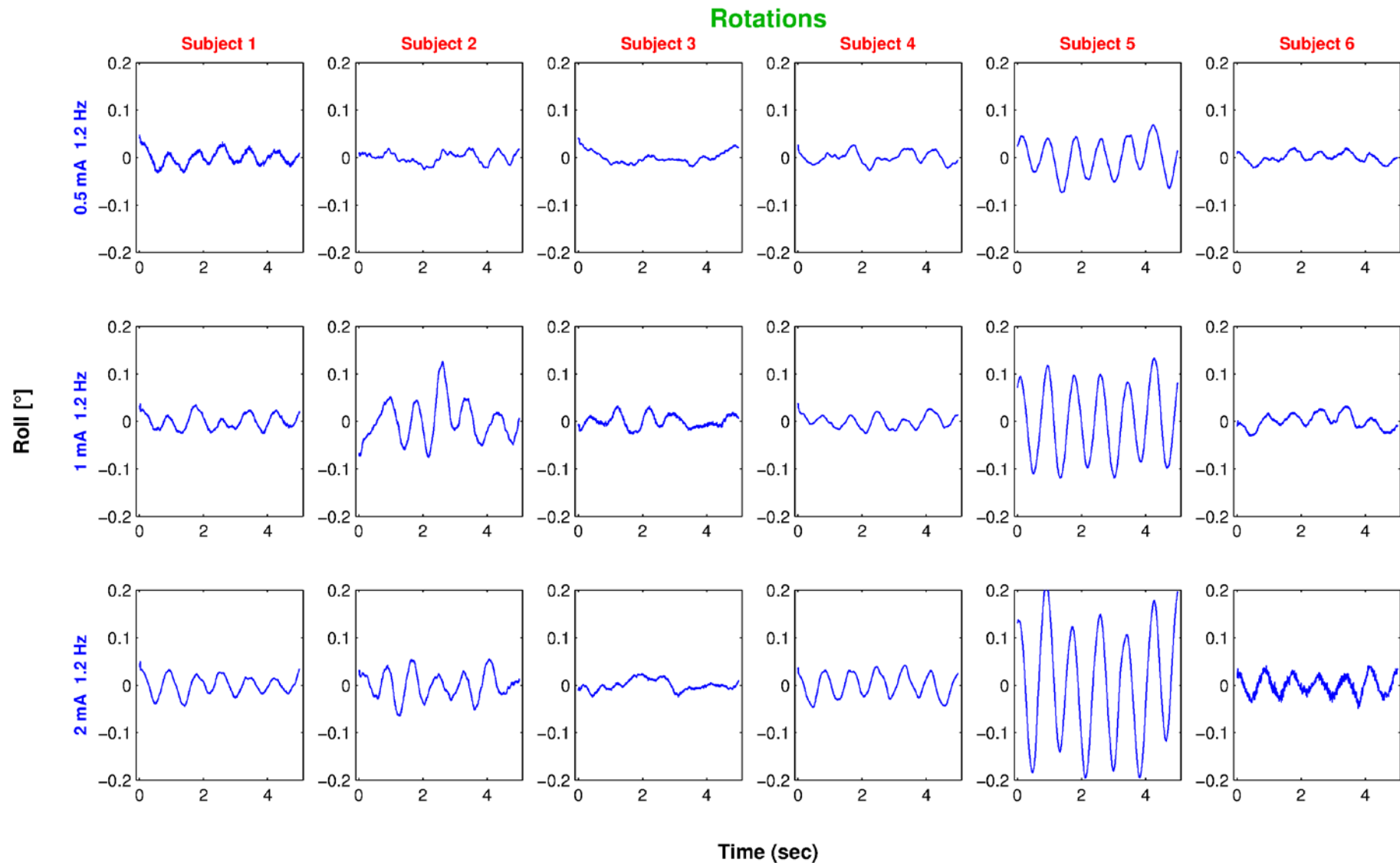


Figure B 1. Averaged roll over segments of 5 seconds for three different amplitudes of 0.5, 1 and 2 mA and frequency of 1.2 Hz

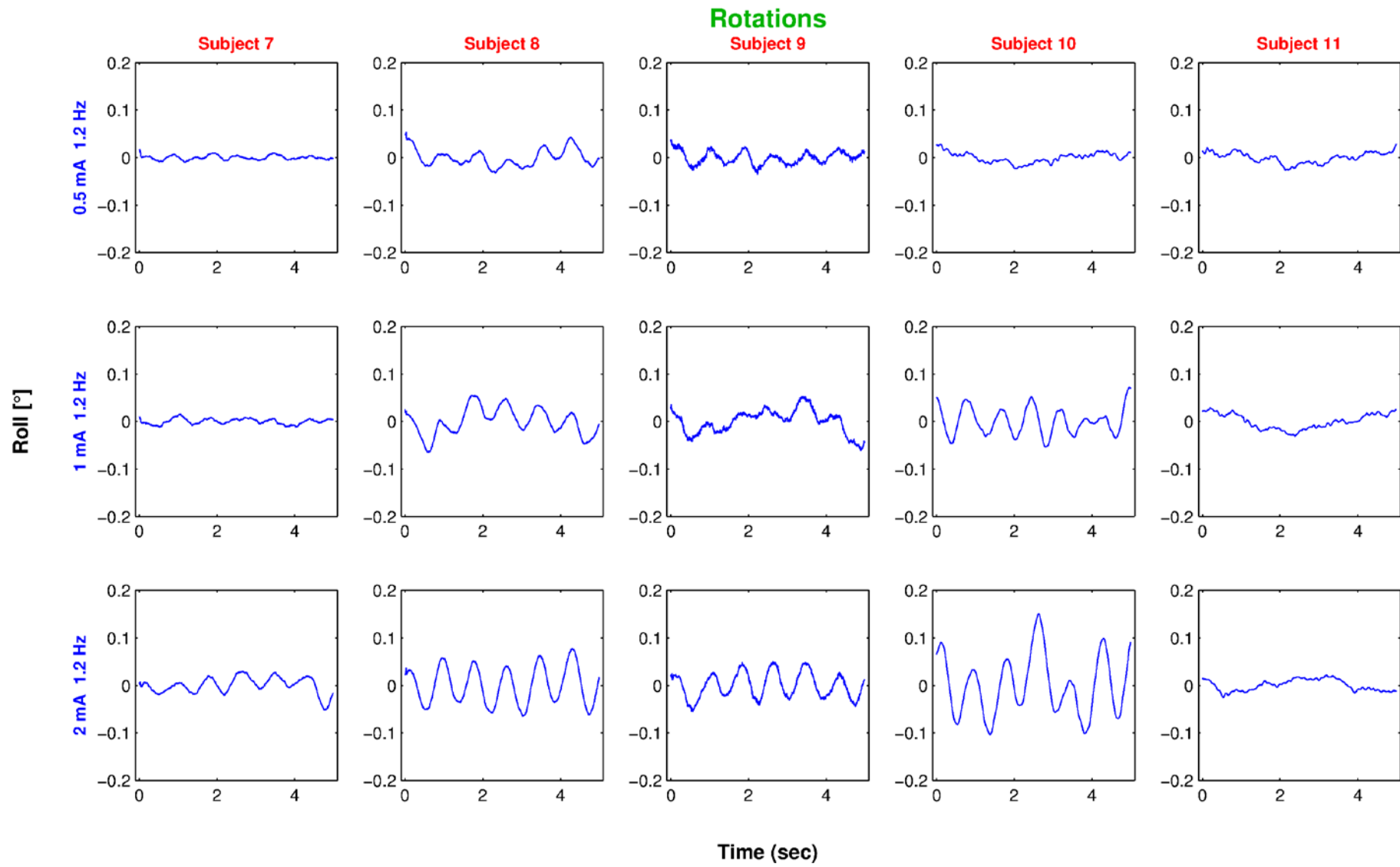


Figure B 2 Averaged roll over segments of 5 seconds for three different amplitudes of 0.5, 1 and 2 mA and frequency of 1.2 Hz

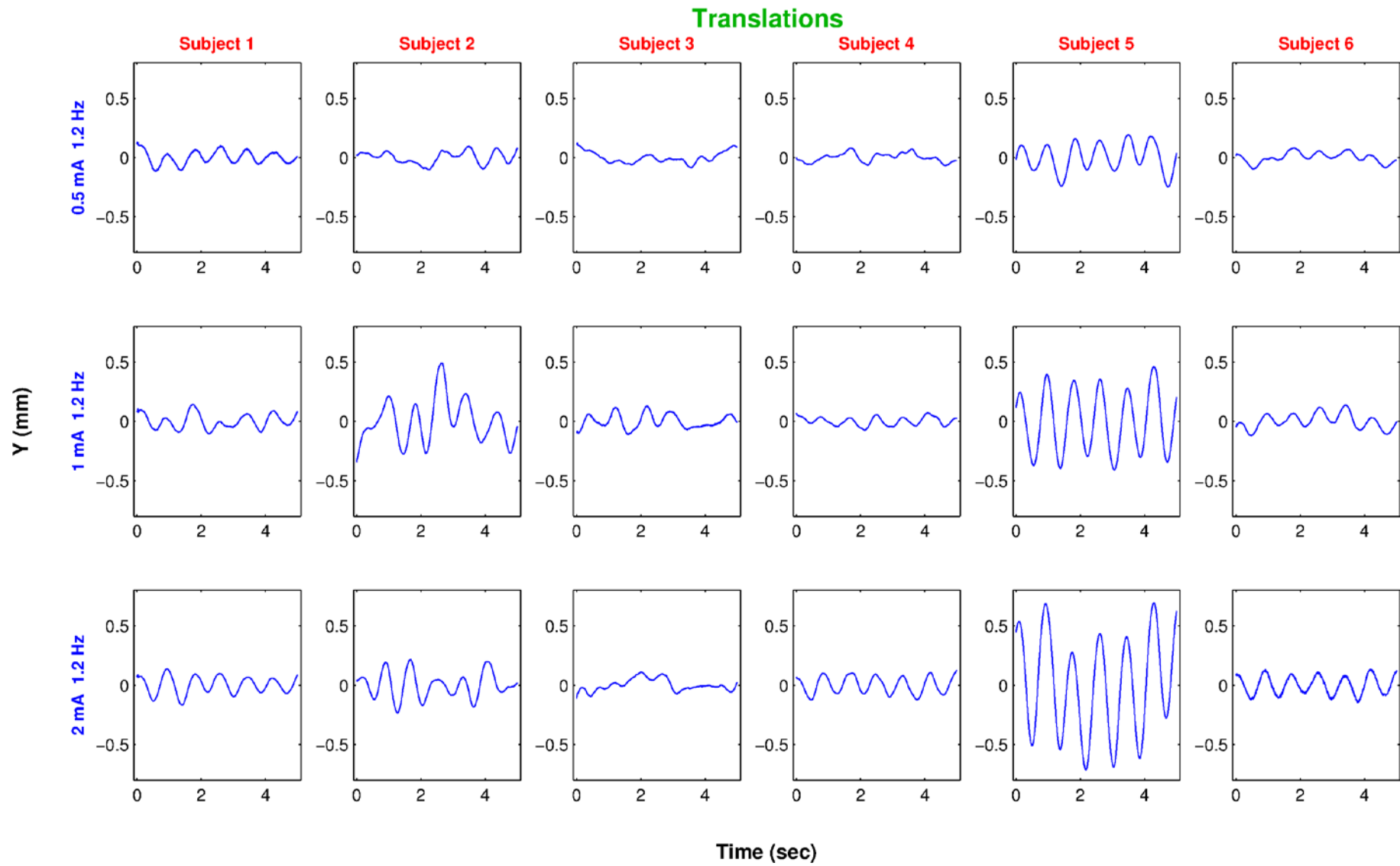


Figure B 3. Averaged Y motion over segments of 5 seconds for three different amplitudes of 0.5, 1 and 2 mA and frequency of 1.2 Hz

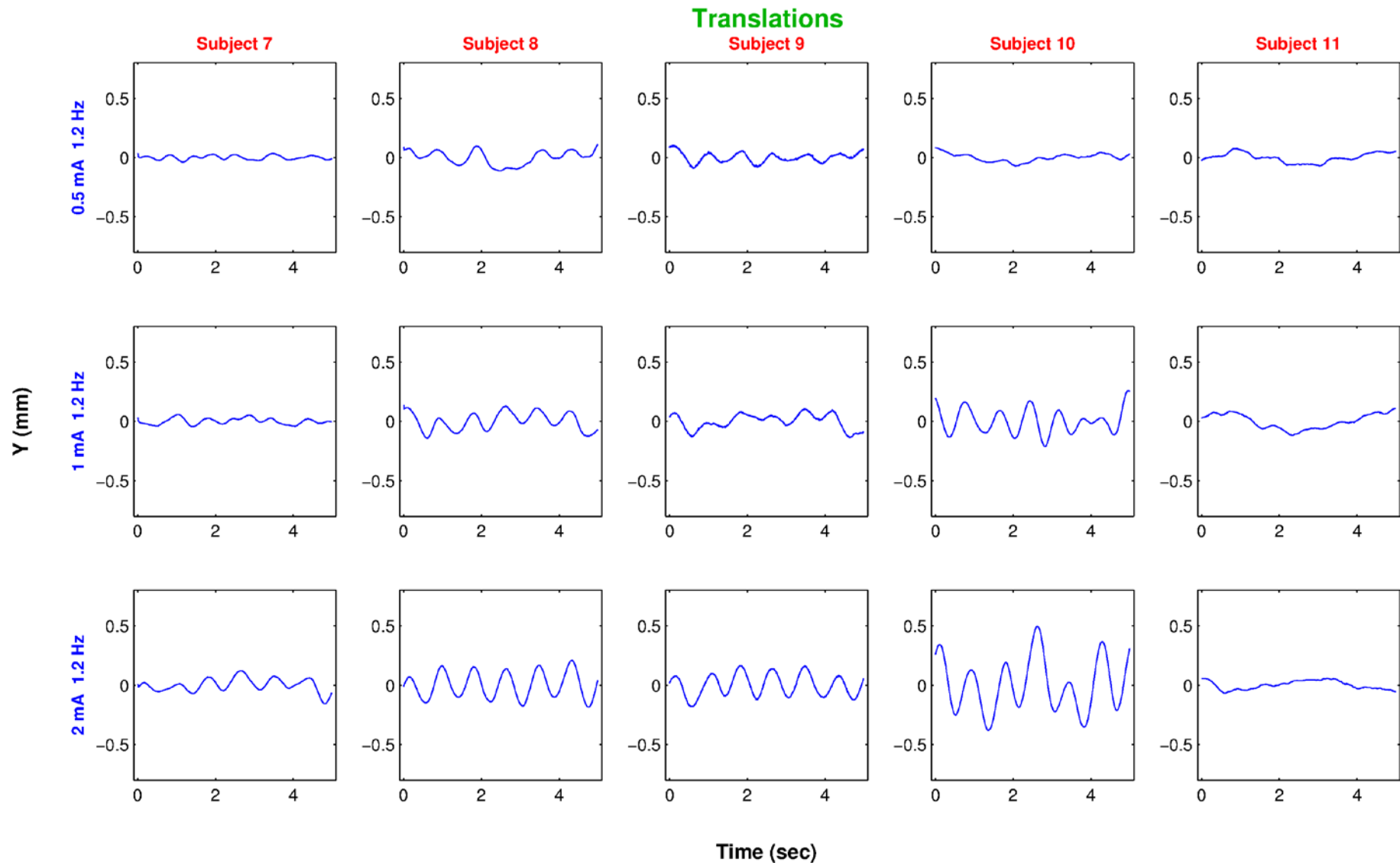


Figure B 4. Averaged Y motion over segments of 5 seconds for three different amplitudes of 0.5, 1 and 2 mA and frequency of 1.2 Hz

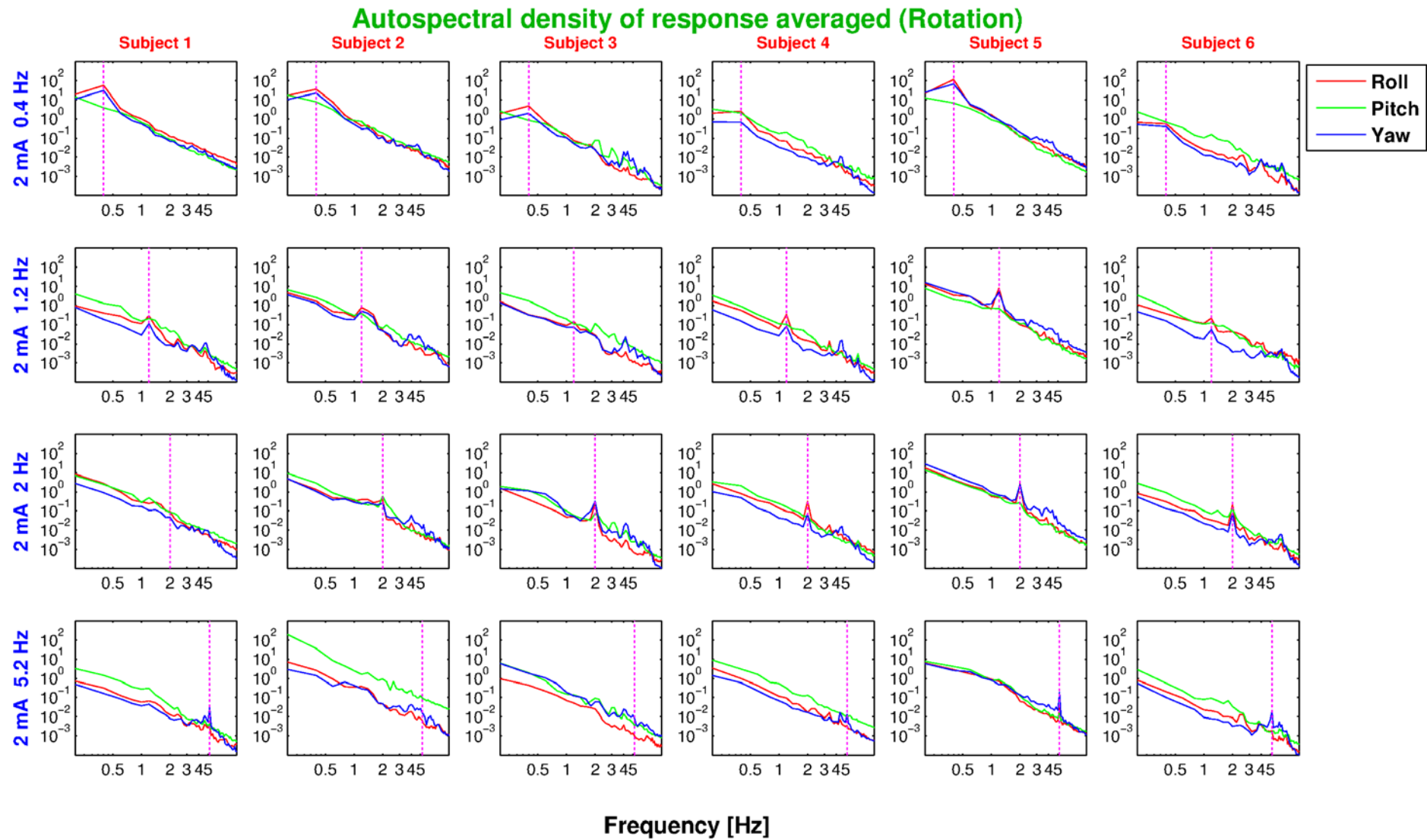


Figure 13. Autospectral densities of responses in rotations for subjects 1-6. Four rows show the data from 0.4,1.2,2 and 5.2 Hz stimuli of 2 mA.

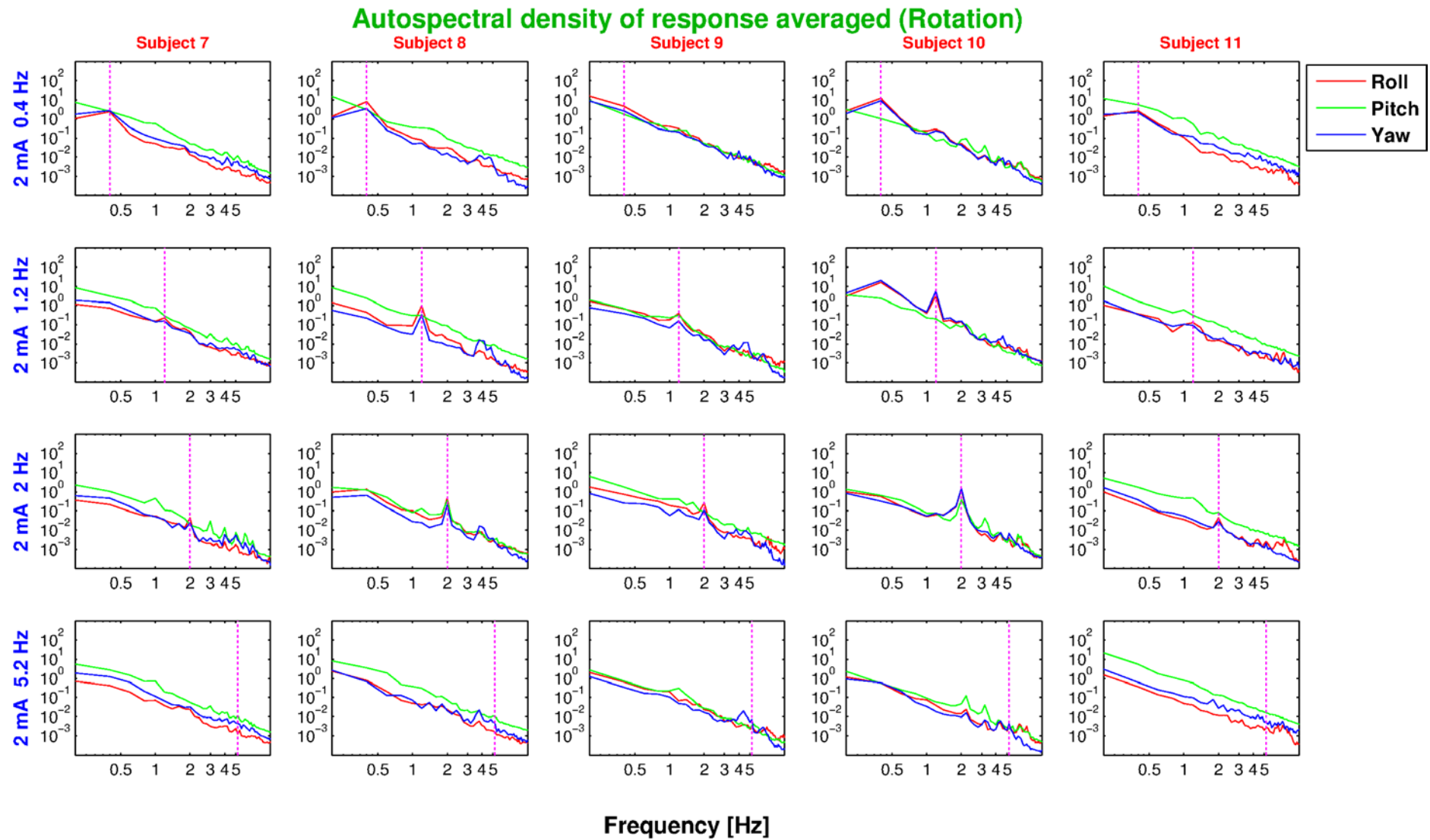


Figure 14. Autospectral densities of responses in rotations for subjects 7-11. Four rows show the data from 0.4, 1.2, 2 and 5.2 Hz stimuli of 2 mA.

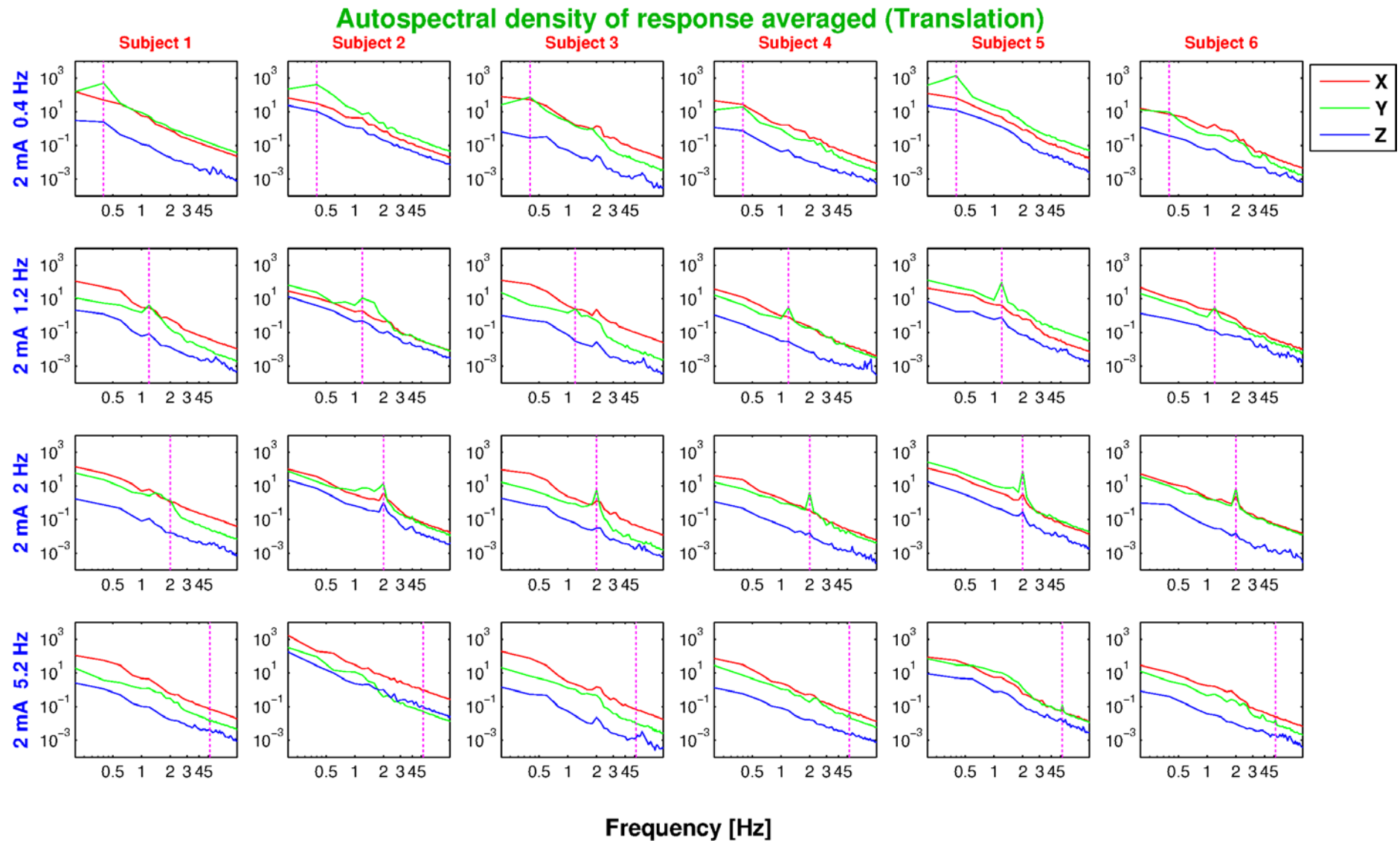


Figure 15. Autospectral densities of responses in translations for subjects 1-6. Four rows show the data from 0.4, 1.2, 2 and 5.2 Hz stimuli of 2 mA.

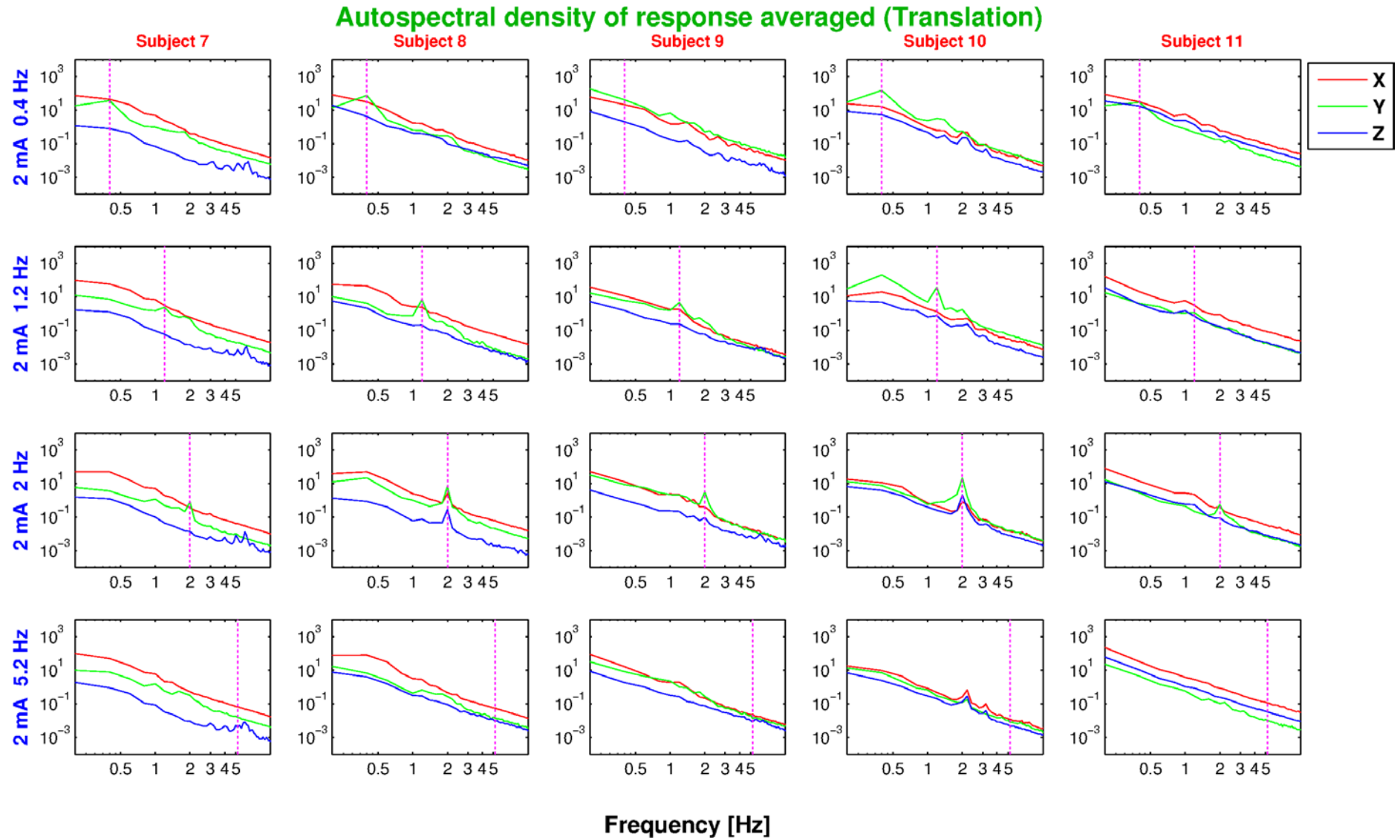


Figure 16. Autospectral densities of responses in translations for subjects 7-11. Four rows show the data from 0.4, 1.2, 2 and 5.2 Hz stimuli of 2 mA.

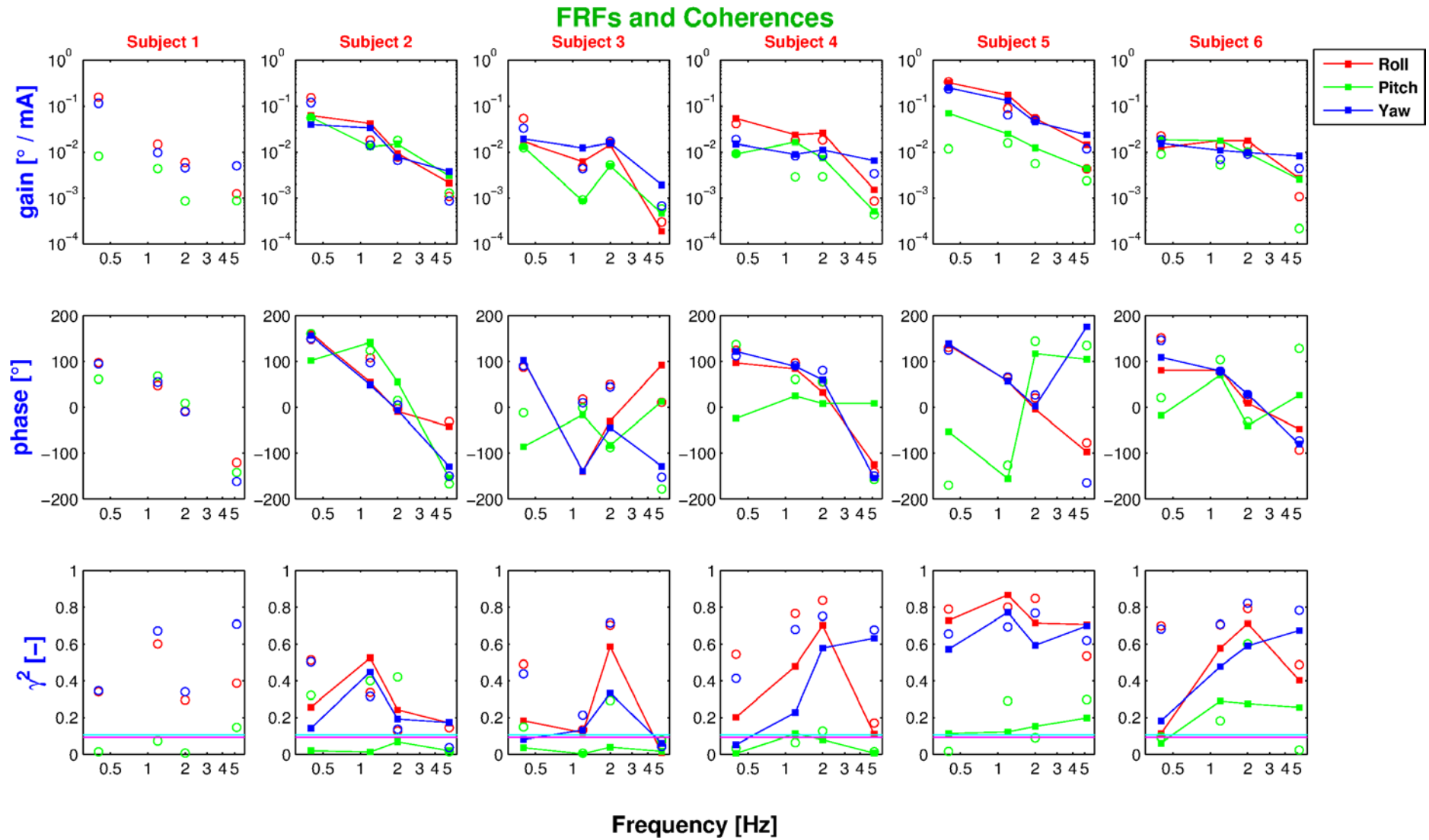


Figure B 5. FRFs and coherences for rotations. Sines from subjects 1-6 are shown with circles and multisines from subjects 2-6 are shown with connected squares.

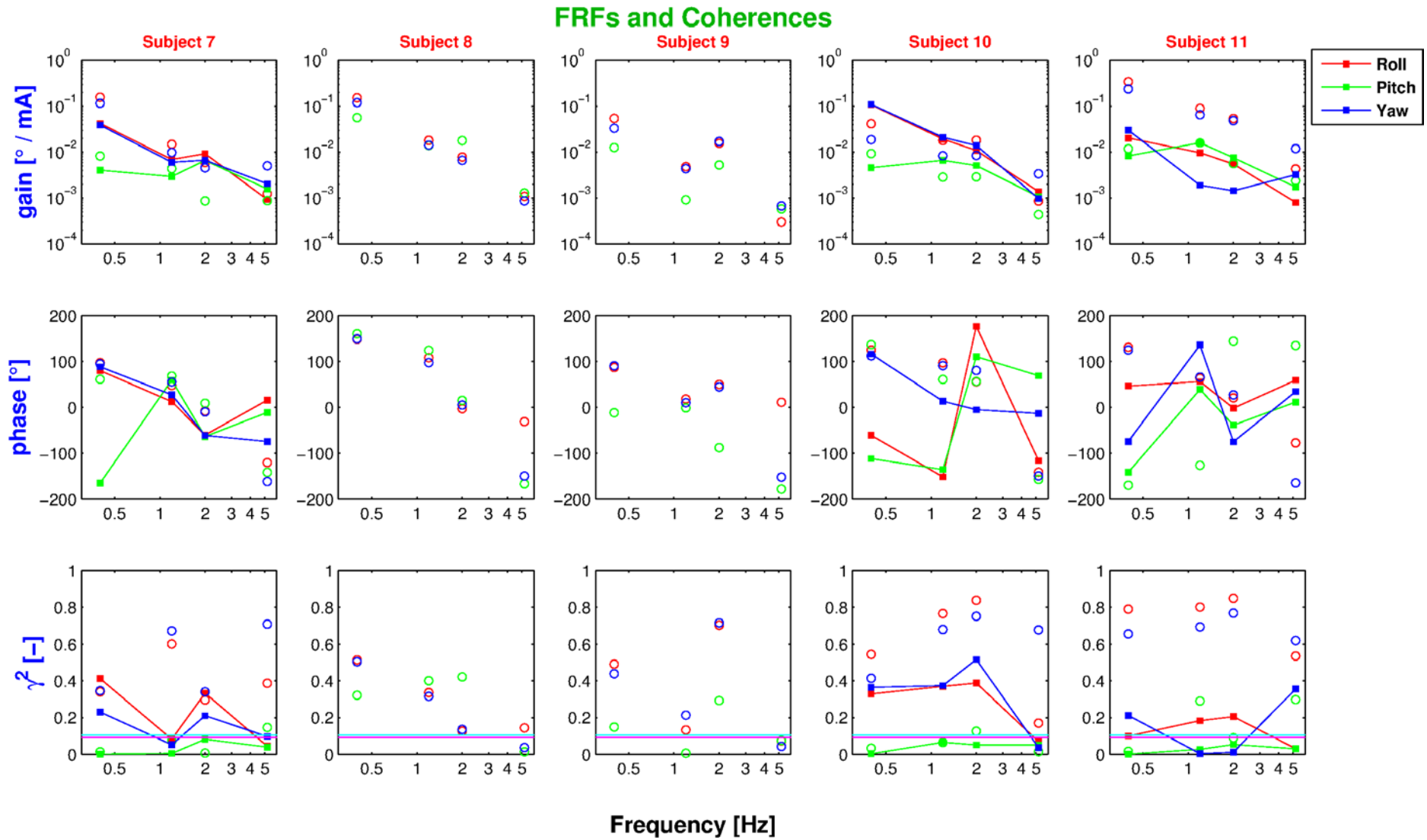


Figure B 6. FRFs and coherences for rotations. Sines and Multisine

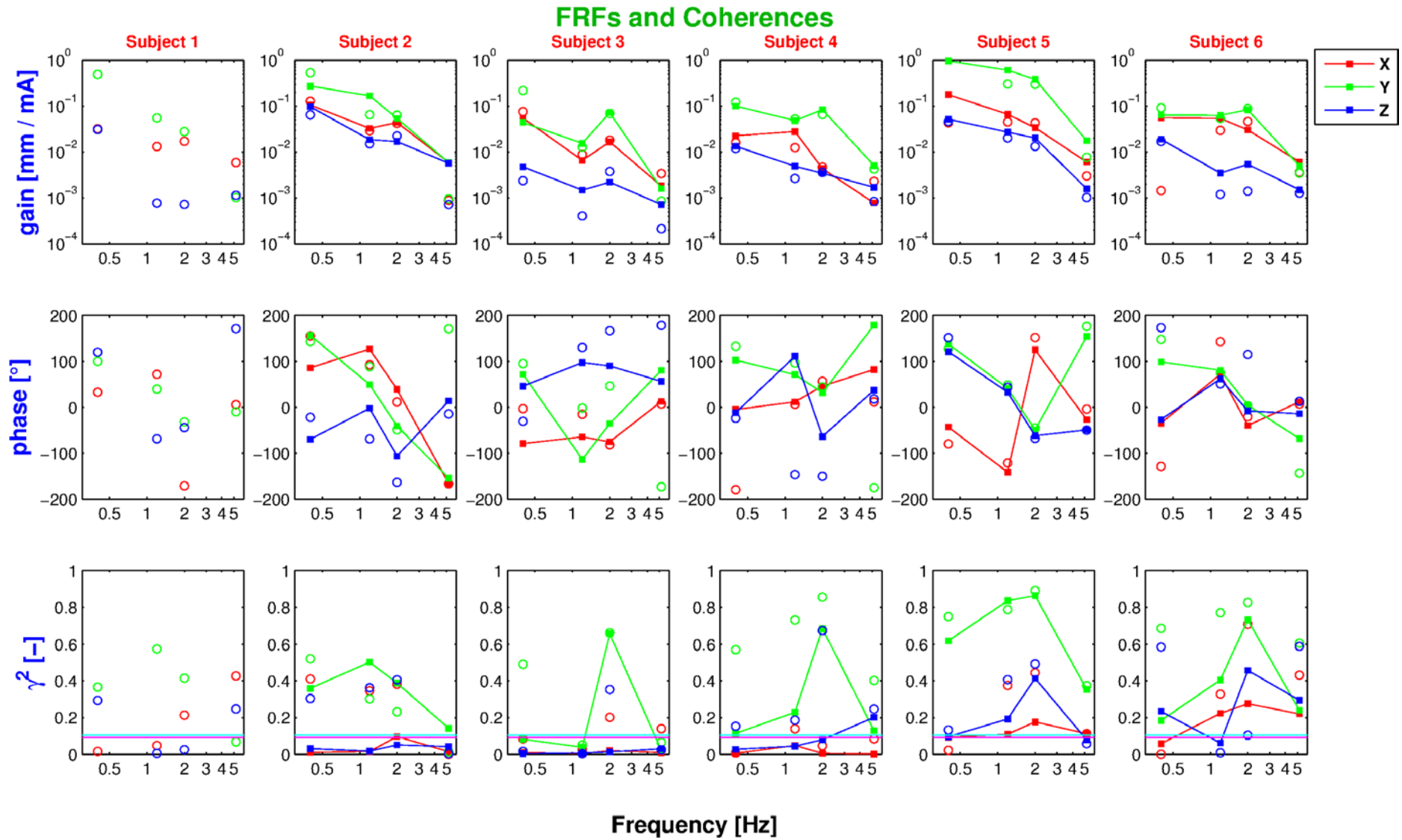


Figure B 7. FRFs and coherences for translations. Sines and Multisine

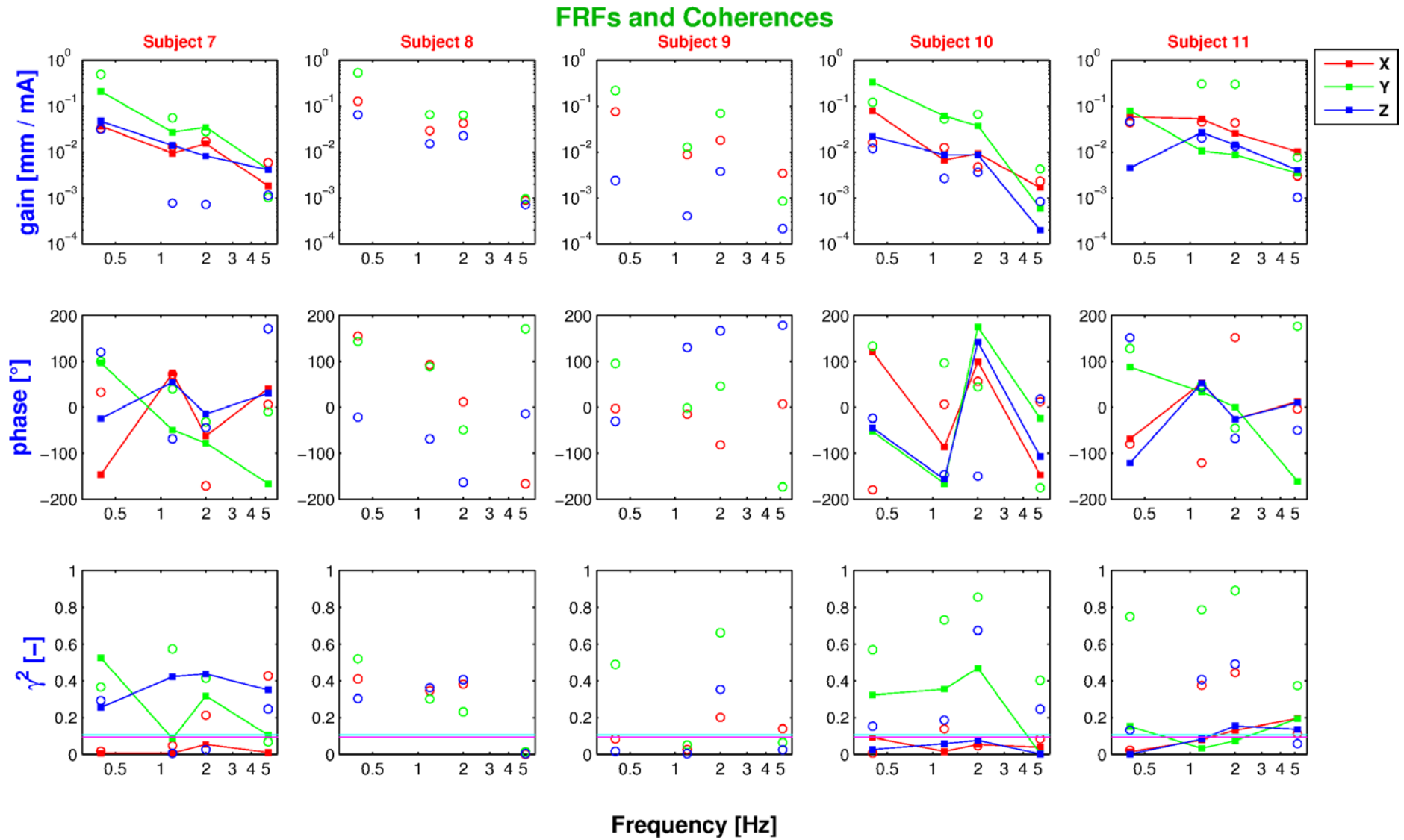


Figure B 8. FRFs and coherences for translations. Sines and Multisine

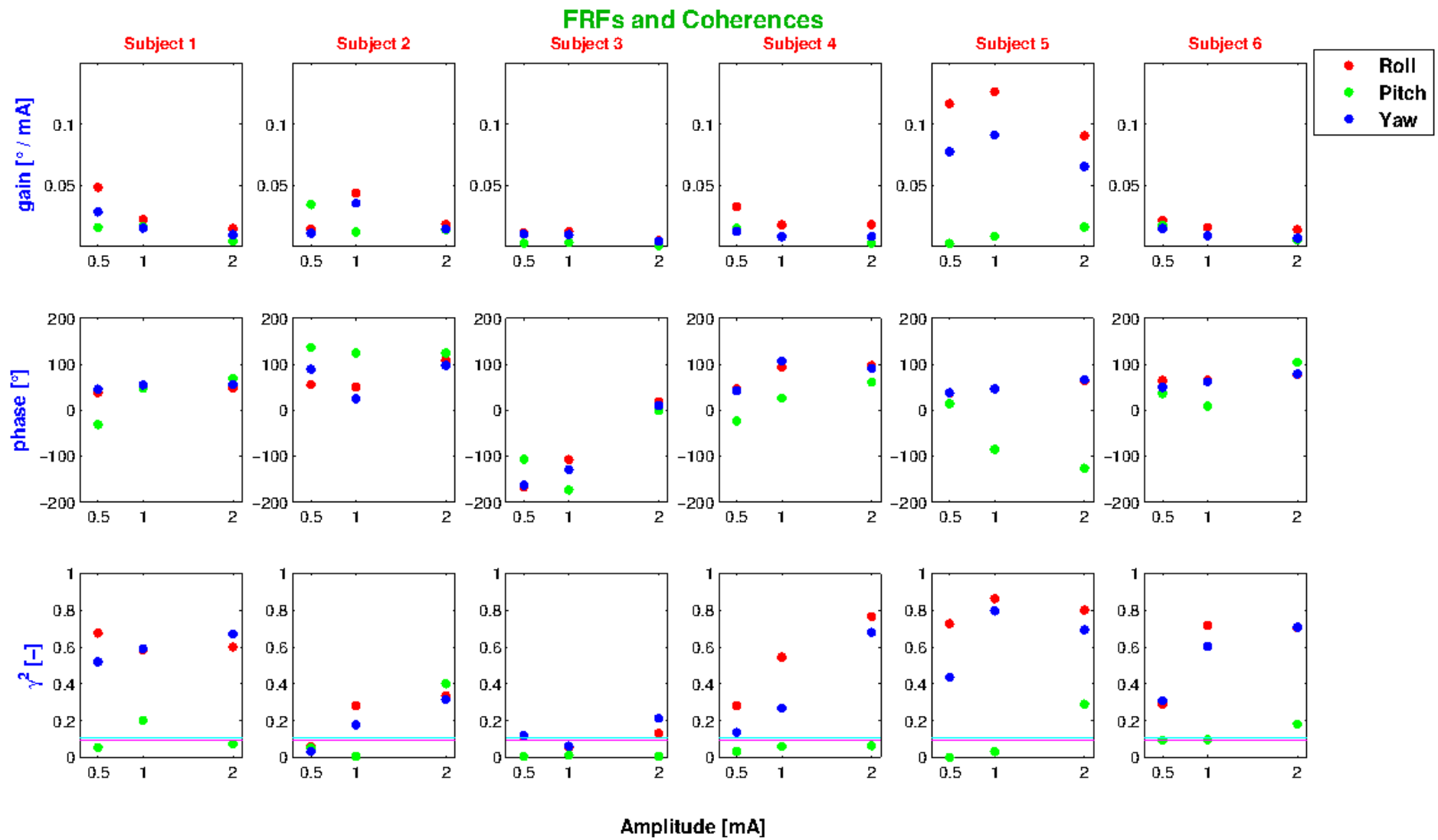


Figure B 9. FRFs and coherences for rotations. Amplitude tests

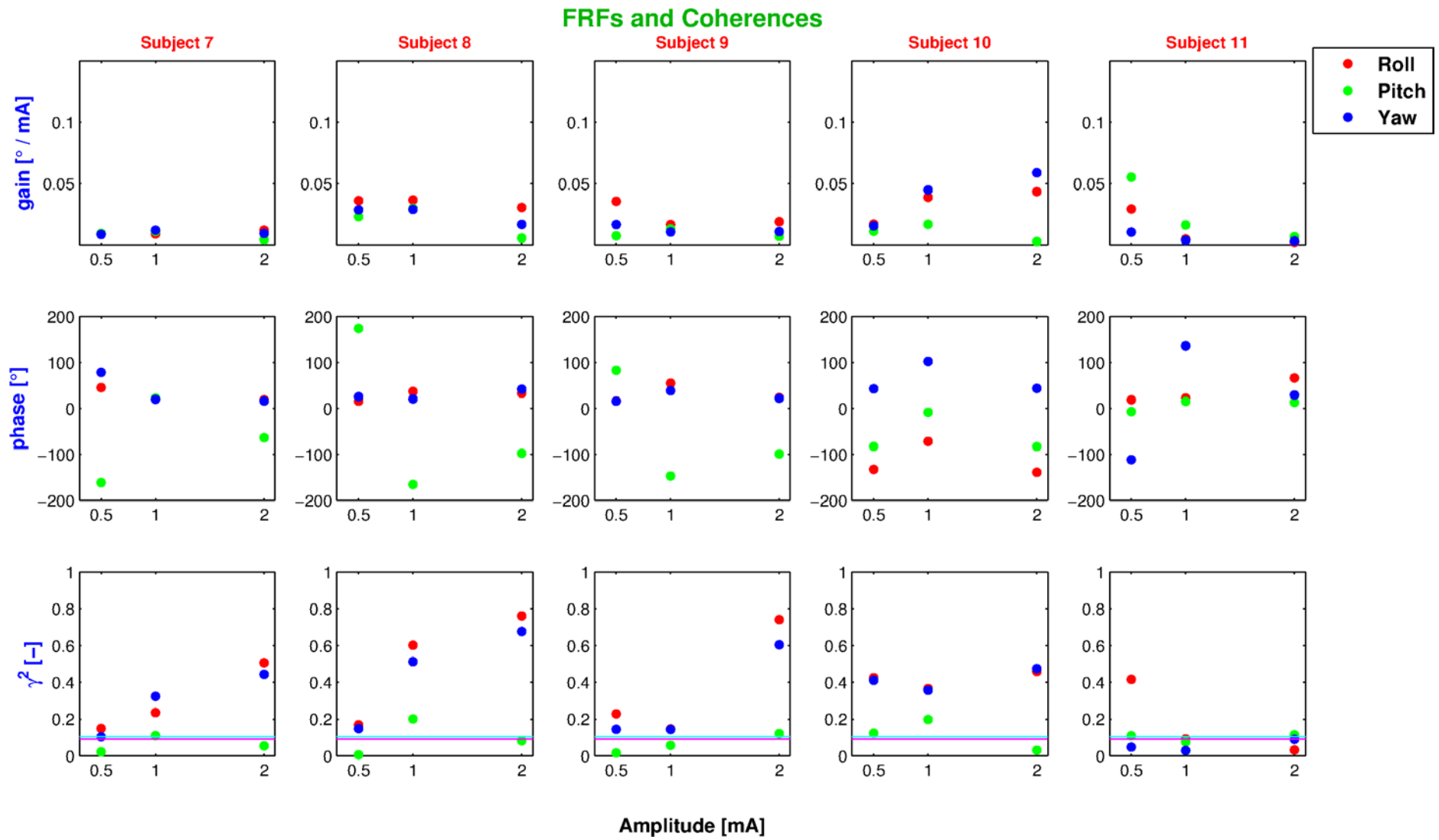


Figure B 10. FRFs and coherences for rotations. Amplitude tests

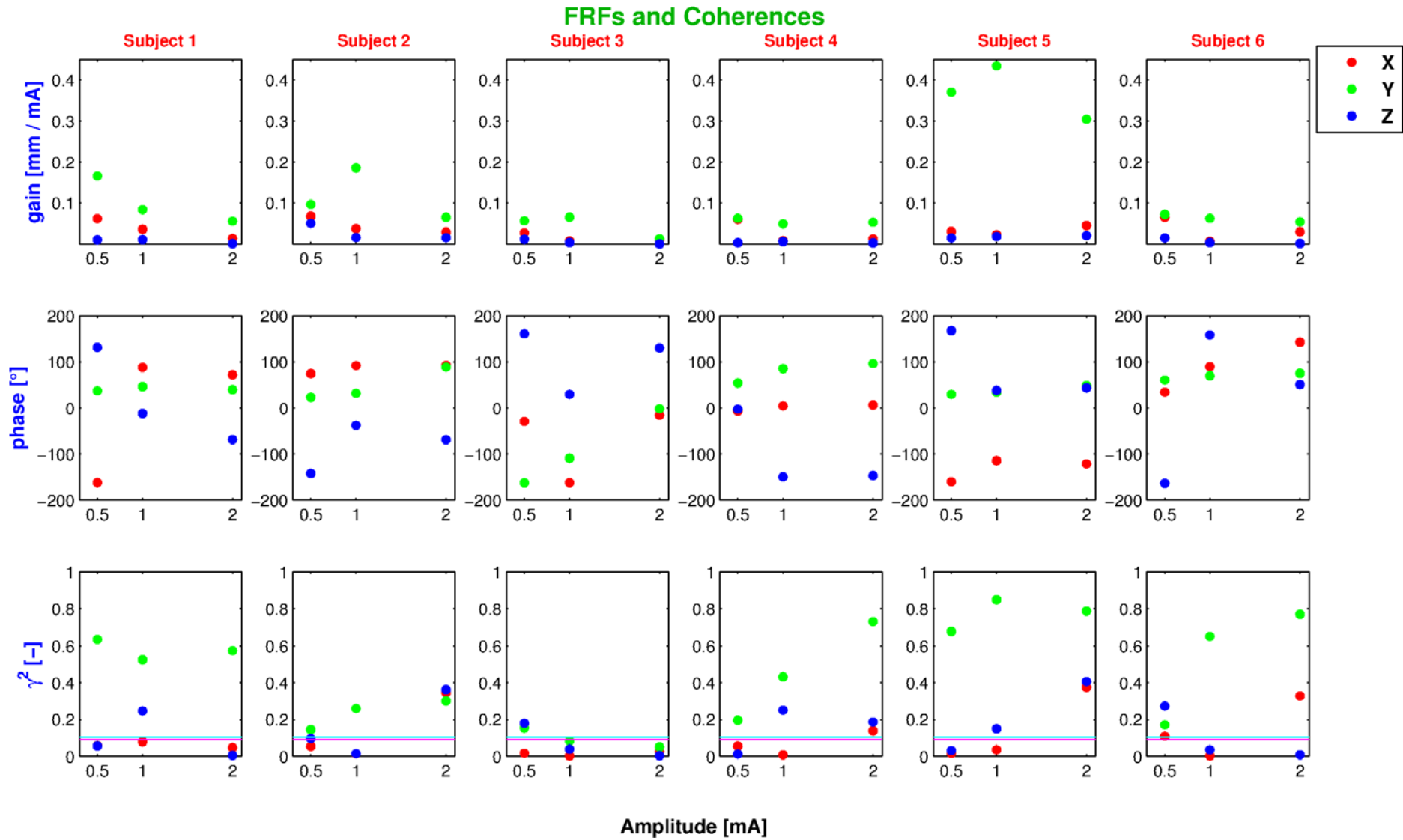


Figure B 11. FRFs and coherences for translations. Amplitude tests

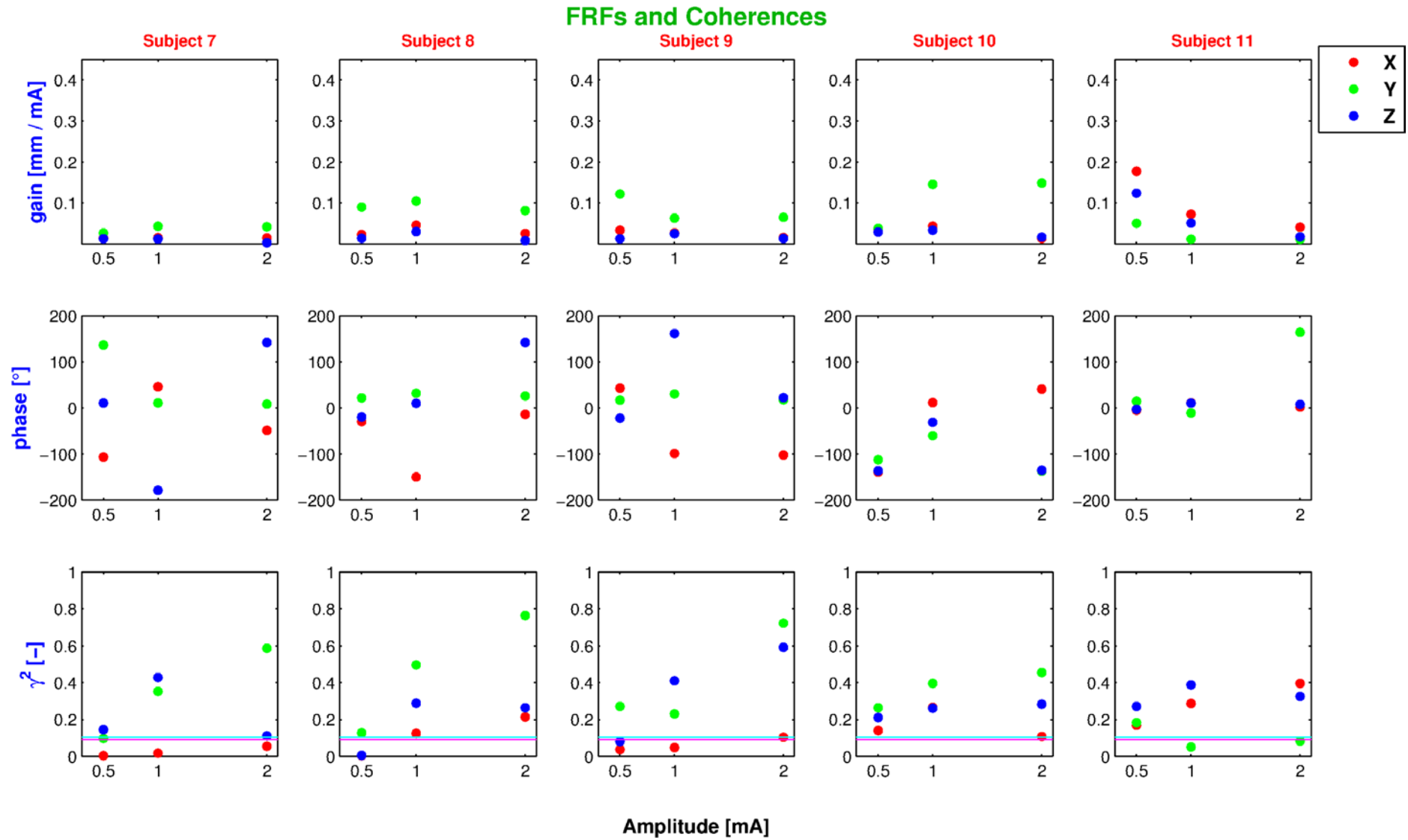


Figure B 12. FRFs and coherences for translations. Amplitude tests

Appendix C – EMG measurements and analysis

EMG measurements and analysis

Investigation of neck muscle activities in response to GVS has been performed in a pilot study with two subjects. EMG data has been collected from four muscles at left body side: Sternocleidomastoid (ST), scalenus (SC), splenius capitis (SP) and trapezius (TR). Signals are recorded using unipolar electrodes with 20 mm distance. Figure C 1 shows the bipolar signals high pass filtered at 30 Hz to remove motion artifacts and low pass filtered at 400 Hz to prevent aliasing. The signal visible in figure is similar to the stimulus for all muscles. Figure C 2 shows zoomed in view of 2 mA 0.4 Hz at its first peak. The EMG signal is now visible. It is observed in the figures that muscle activity is buried under GVS artifact. To remove this artifact we subtracted the stimulus from the recorded signals in time domain and applied spectral analysis to find out if this approach can reveal the muscle activities behind the observed coherent motions.

Figure C 3 shows auto power spectra for four muscles after subtracting the GVS signals from EMG signals. It is observed in the figure that data does not show significant stimulation power at the four frequency points. There are some points which have dominant power compared to adjacent points but several other non stimulated points show more power across the spectra. At 0.4 Hz where the most sway is observed the sternocleidomastoid which always has strong activities does not show any dominant power. Also power is observed at harmonics of stimuli due the artifact. The data from splenius capitis shows this effect substantially since this muscle was very close to stimulation site. This means that subtraction of stimulus from EMG could not result in revealing the muscle activities related to the observed motions. Two possible causes might be attributed to this problem. First possibility is that by removing the stimulus in subtraction method, the EMG power is also removed. The second possibility is that surface EMG could not successfully capture the activity in muscles. It might be that the signal is coming from deep muscles and not the superficial muscles. This results in poor sEMG SNR. For further exploration on this matter we propose to apply more advanced techniques in signal decomposition such as principal component analysis or wavelet technique as they are in use by some researchers in artifact removal of some biomedical signals like ECG. Another alternative approach in research could be the use of other measurement techniques such as wire EMG recording. This technique could eliminate the superficial noise substantially and record the activity from deep muscles. While the sEMG does not show significant power at the applied stimulus frequencies, apparent effects of GVS can be seen in comparison to the NHS condition. Stimuli at 0.4 Hz, 1.2 Hz and multisine result in increased EMG in sternocleidomastoid, scalenus and splenius. No effects of GVS are observed in the Trapezius. This could be attributed to the fact that trapezius is not located at the neck and has a further distance to other neck muscles. As a result the activity of this muscle is more prone to noise. A close look of the raw data showed ECG signal captured in recordings from trapezius. This reveals a low SNR for this muscle.

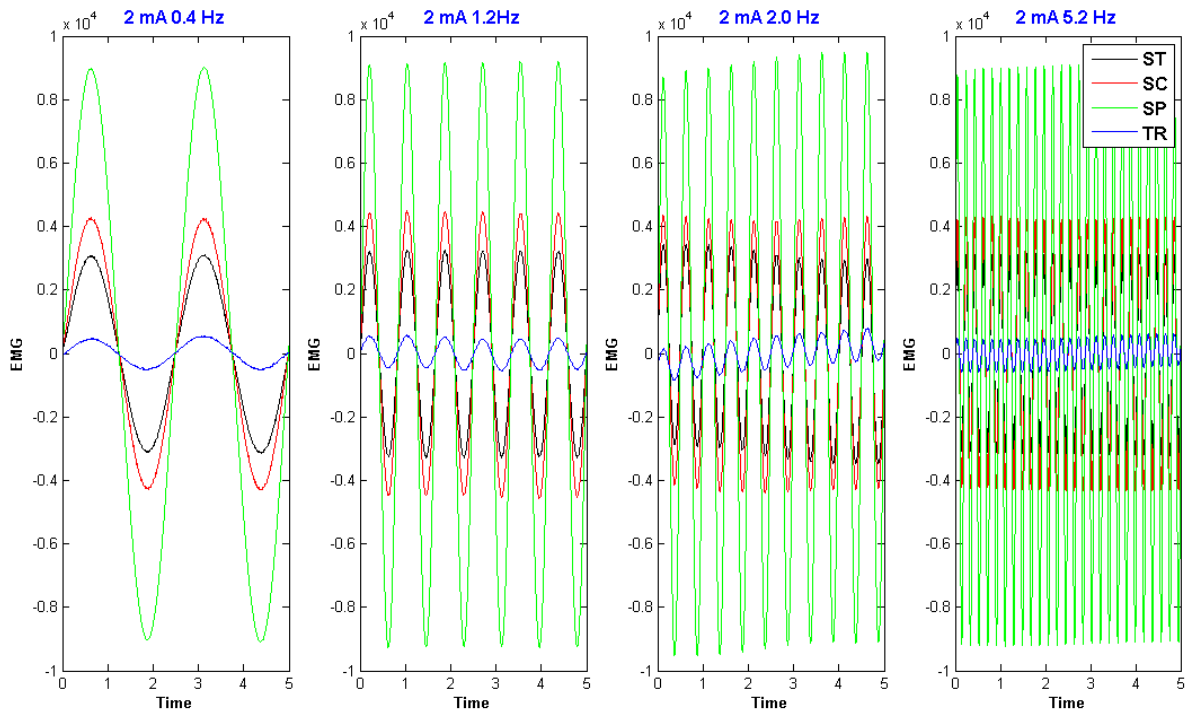


Figure C 1. EMG data high pass filtered for four muscles in 2 mA single sines stimuli. Sternocleidomastoid (ST), Scalenus (SC), Splenius capitis (SP), Trapezius (TR)

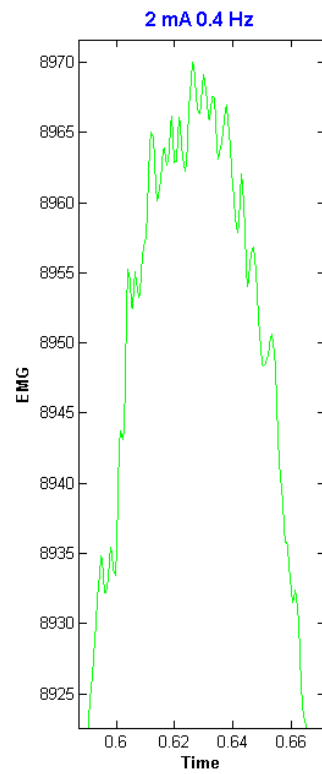


Figure C 2. Zoomed in view of first peak for 2mA 0.4 Hz stimulus

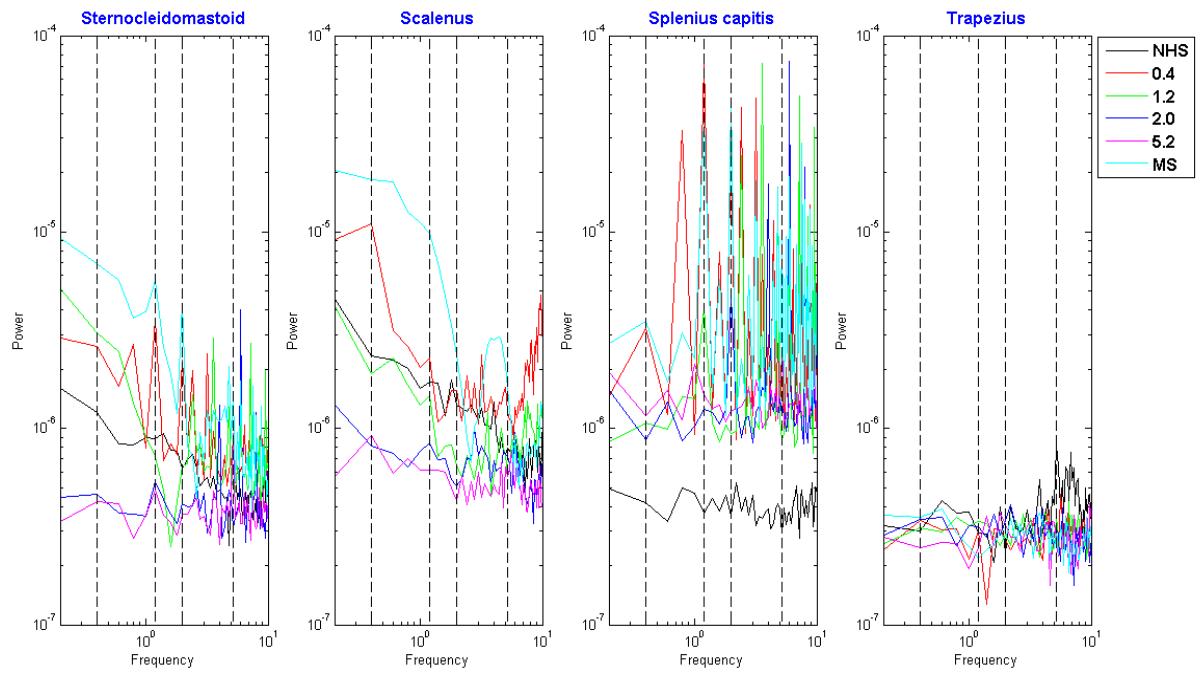


Figure C 3. Auto spectral densities of EMG from four muscles in NHS, four single sines and multisine